Mathematical Models and Numerical Methods for Compressible Multicomponent Flow

Keh-Ming Shyue

Department of Mathematics

National Taiwan University

What is Multiphase Flow ?

- General features
  - Existence of more than one phase or component (fluid-like or not) in an underlying flow environment separated by interfaces
- Problems of interest
  - Wave dynamics with interfaces

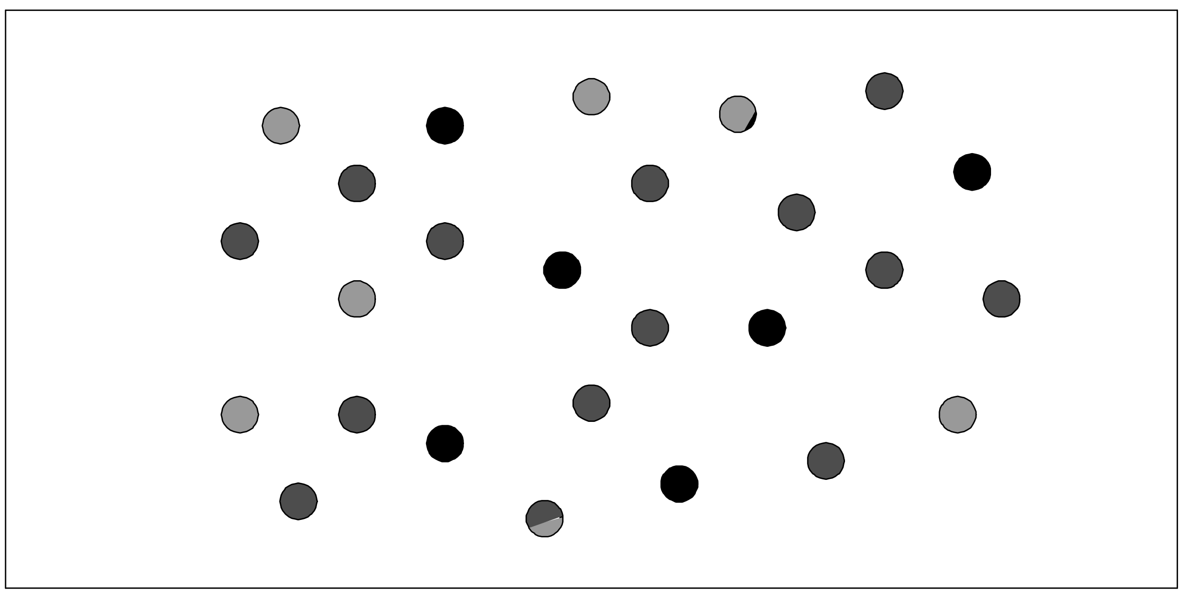

Typical Multiphase Flow Patterns

- Examples taken from Fundamentals of Multiphase Flow, C. E. Brennen, Cambridge, 2005

Typical Multiphase Flow Patterns

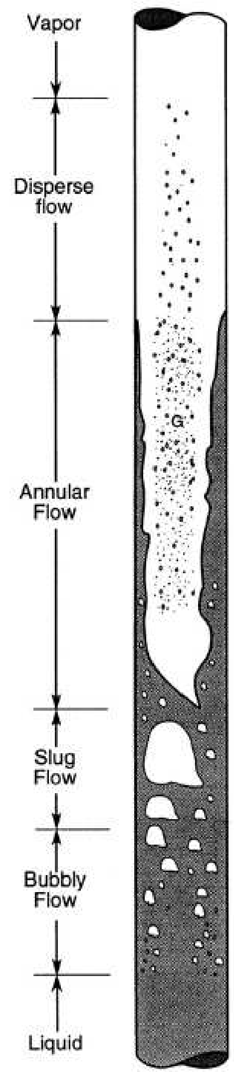

Figure 7.10. The evolution of the steam/water flow in a vertical boiler tube.

Typical Multiphase Flow Patterns

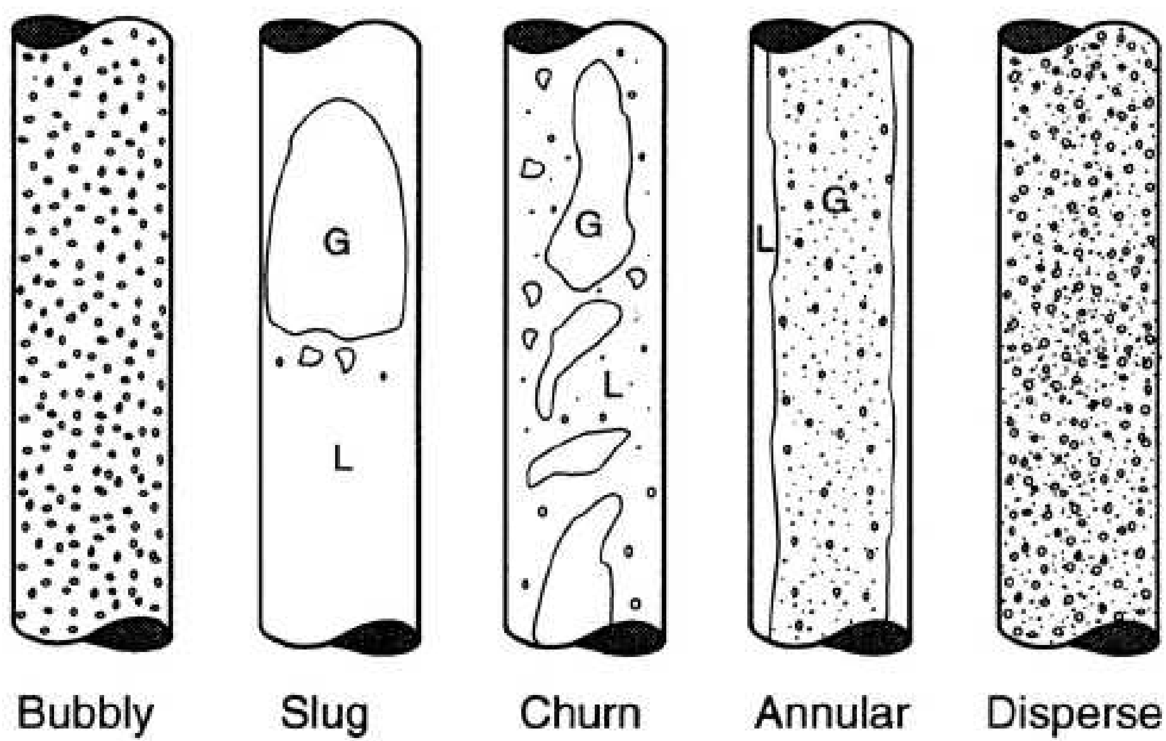

Figure 7.7. Sketches of flow regimes for two-phase flow in a vertical pipe. Adapted from Weisman (1983).

Typical Multiphase Flow Patterns

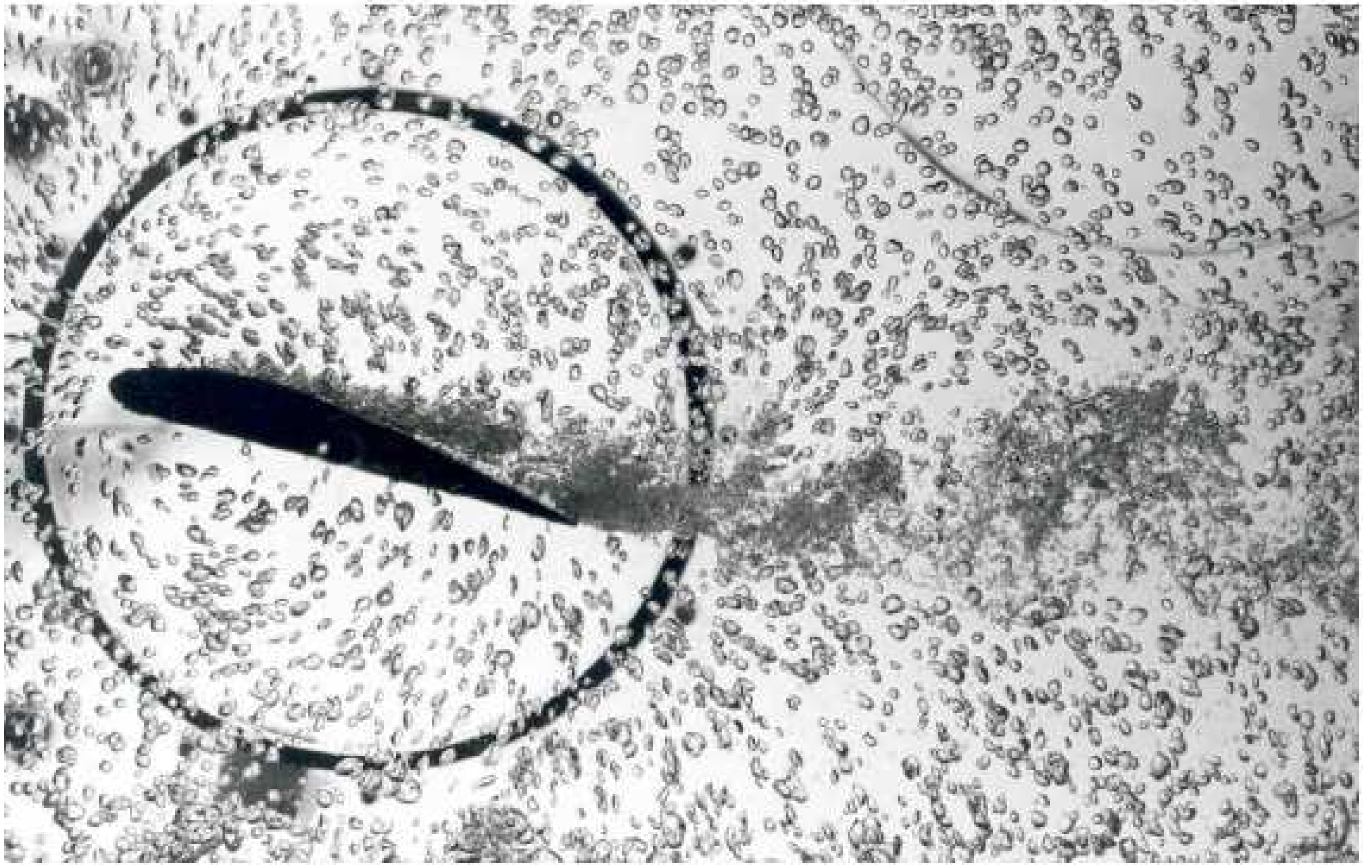

Figure 7.11. Bubbly flow around a NACA 4412 hydrofoil (10cm chord) at an angle of attack; flow is from left to right. From the work of Ohashi *et al.*, reproduced with the author's permission.

Typical Multiphase Flow Patterns

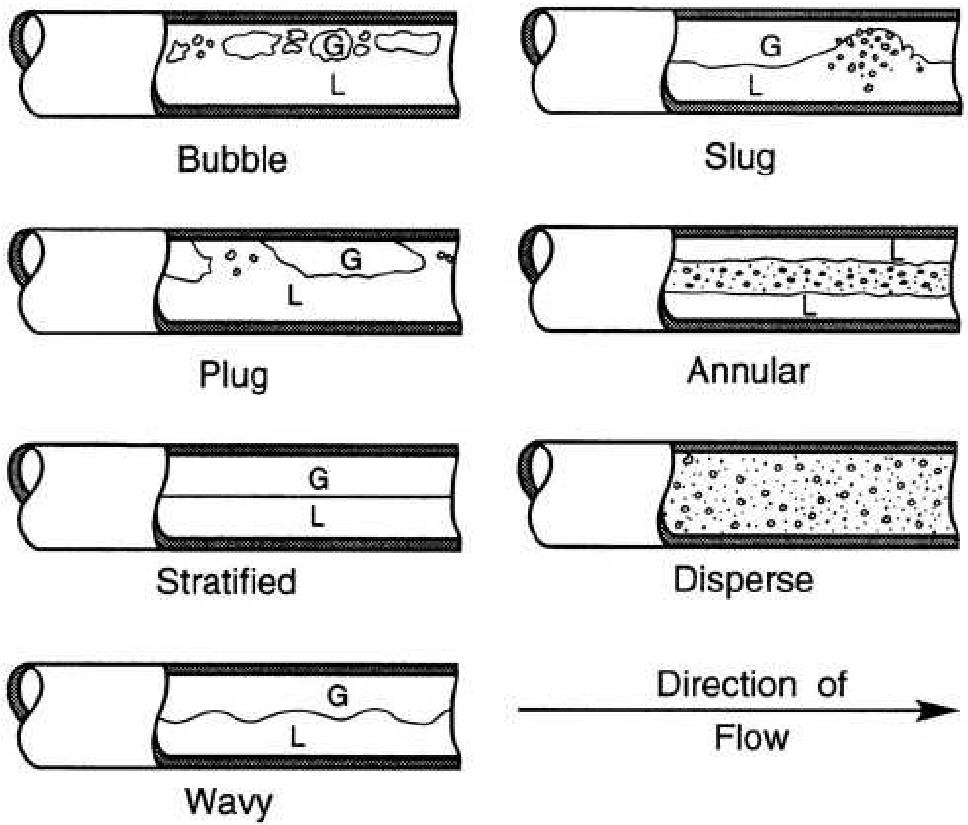

Figure 7.2. Sketches of flow regimes for flow of air/water mixtures in a horizontal, 5.1cm diameter pipe. Adapted from Weisman (1983).

Typical Multiphase Flow Patterns

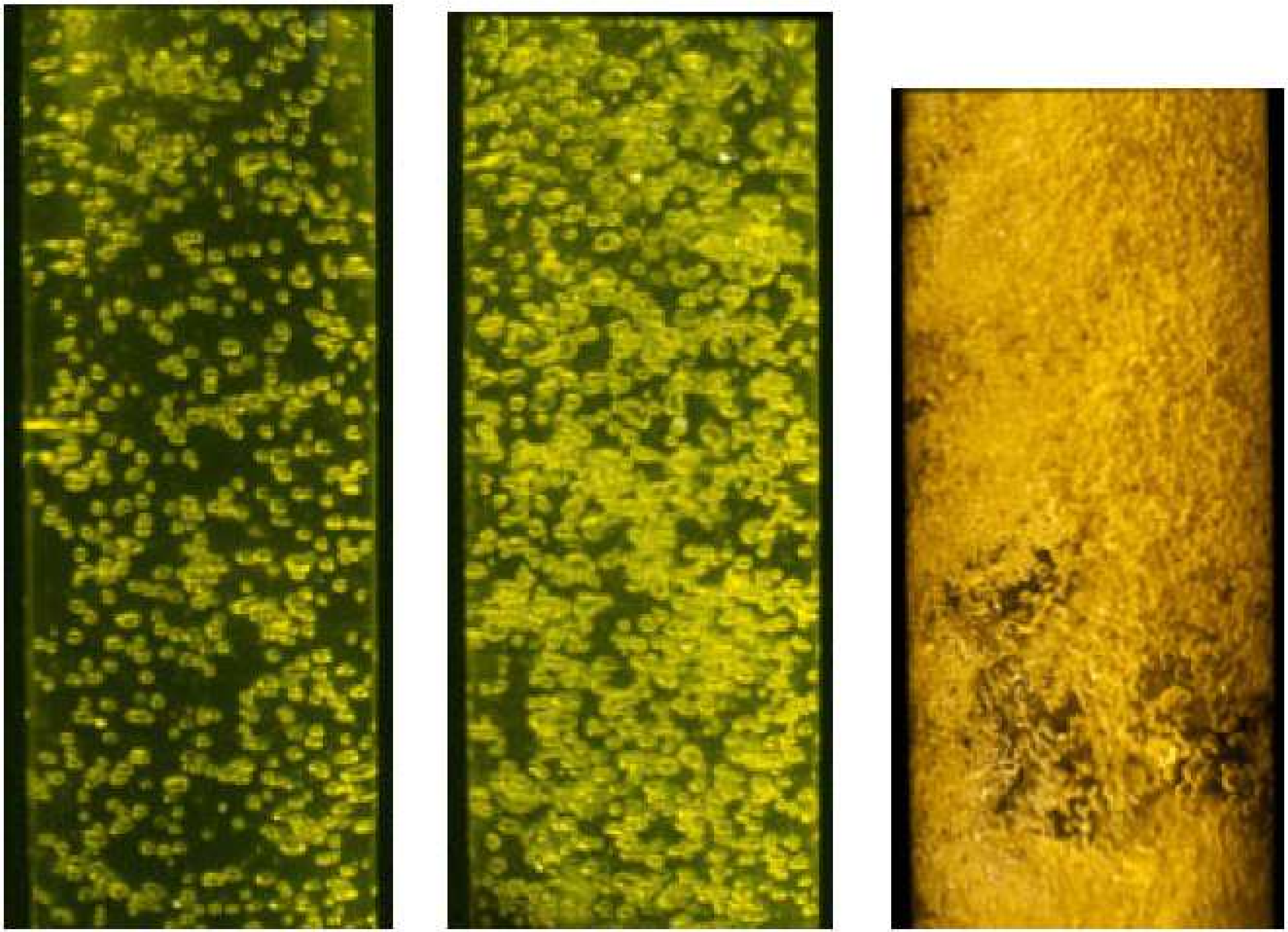

Figure 7.9. Photographs of air/water flow in a 10.2cm diameter vertical pipe (Kytömaa 1987). Left: 1% air; middle: 4.5% air; right: $>$ 15% air.

Typical Multiphase Flow Patterns

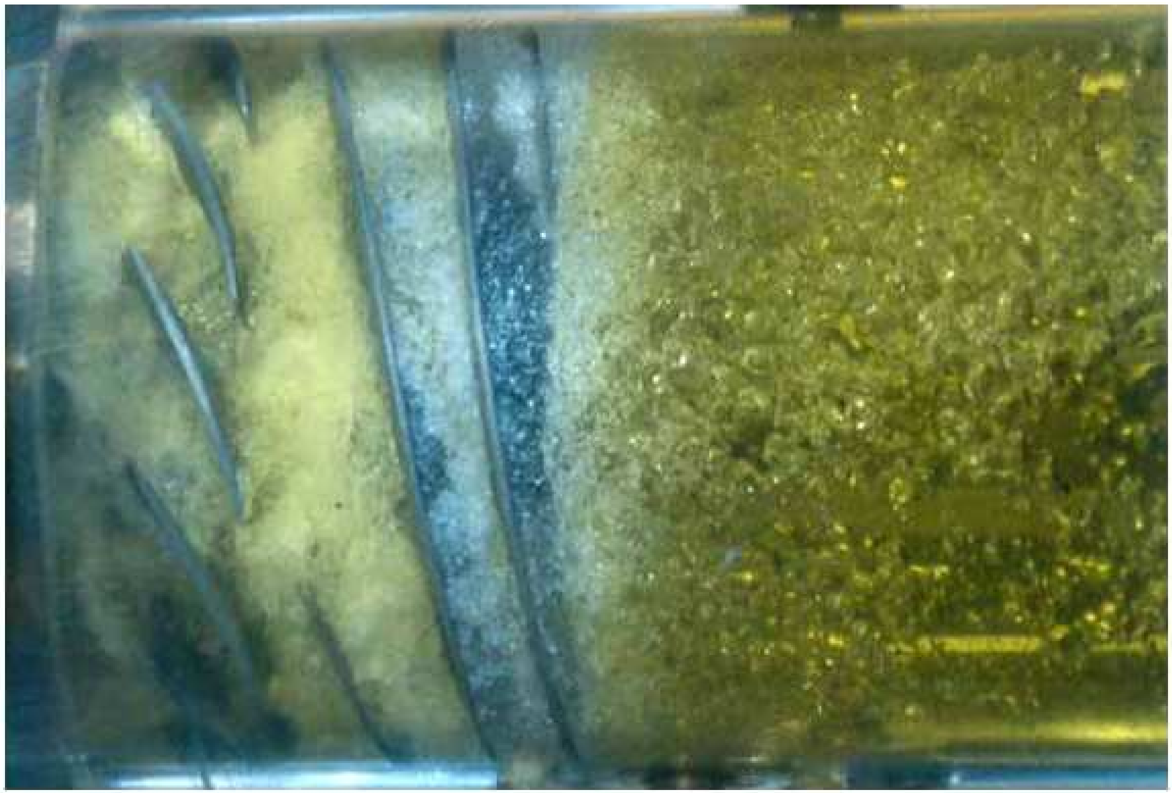

Figure 7.12. A bubbly air/water mixture (volume fraction about 4%) entering an axial flow impeller (a 10.2cm diameter scale model of the SSME low pressure liquid oxygen impeller) from the right. The inlet plane is roughly in the center of the photograph and the tips of the blades can be seen to the left of the inlet plane.

Solid Plate Impact

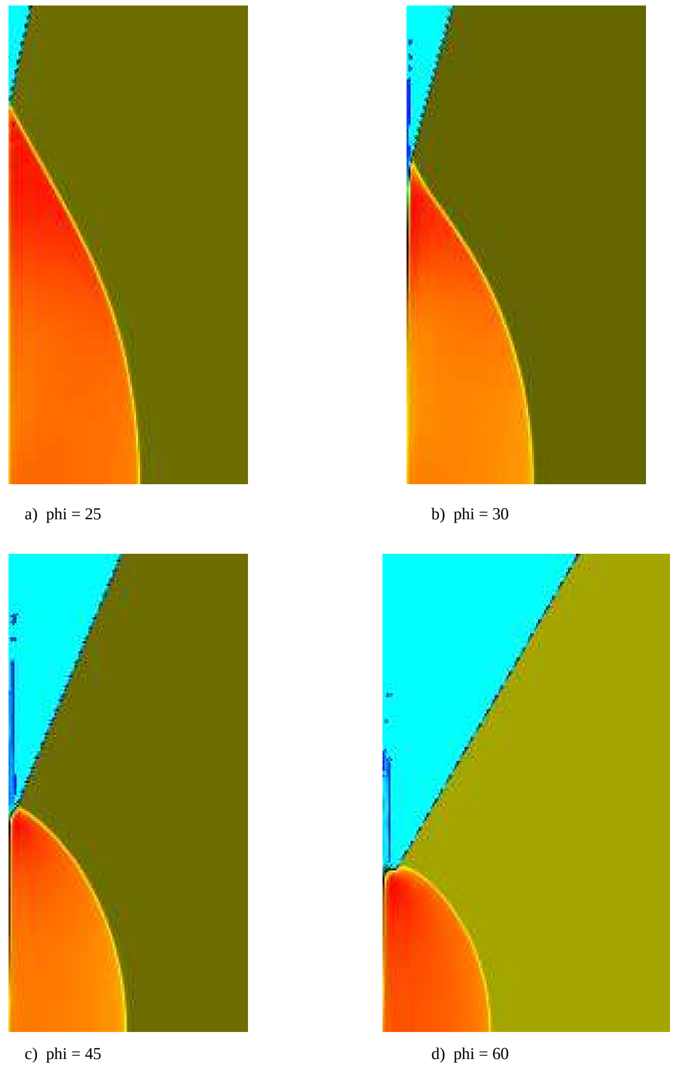

The collision of two aluminum plates inclined at an angle of phi degrees to one another. Only the plate on the right is shown, the left hand boundary is the line of impact. Color contours of density are shown: pale blue is vacuum, green is unshocked aluminum, and dark blue is jetted material. Note that the onset of jetting occurs between phi = 25 and phi = 30 degrees. These computations are of the experiments reported by J.M. Walsh, R.G. Shreffler and F.J. Willig in "Limiting Conditions for Jet Formation in High Velocity Collisions", J. Appl. Phys. 24:349--359 (1953).

Underwater Explosions

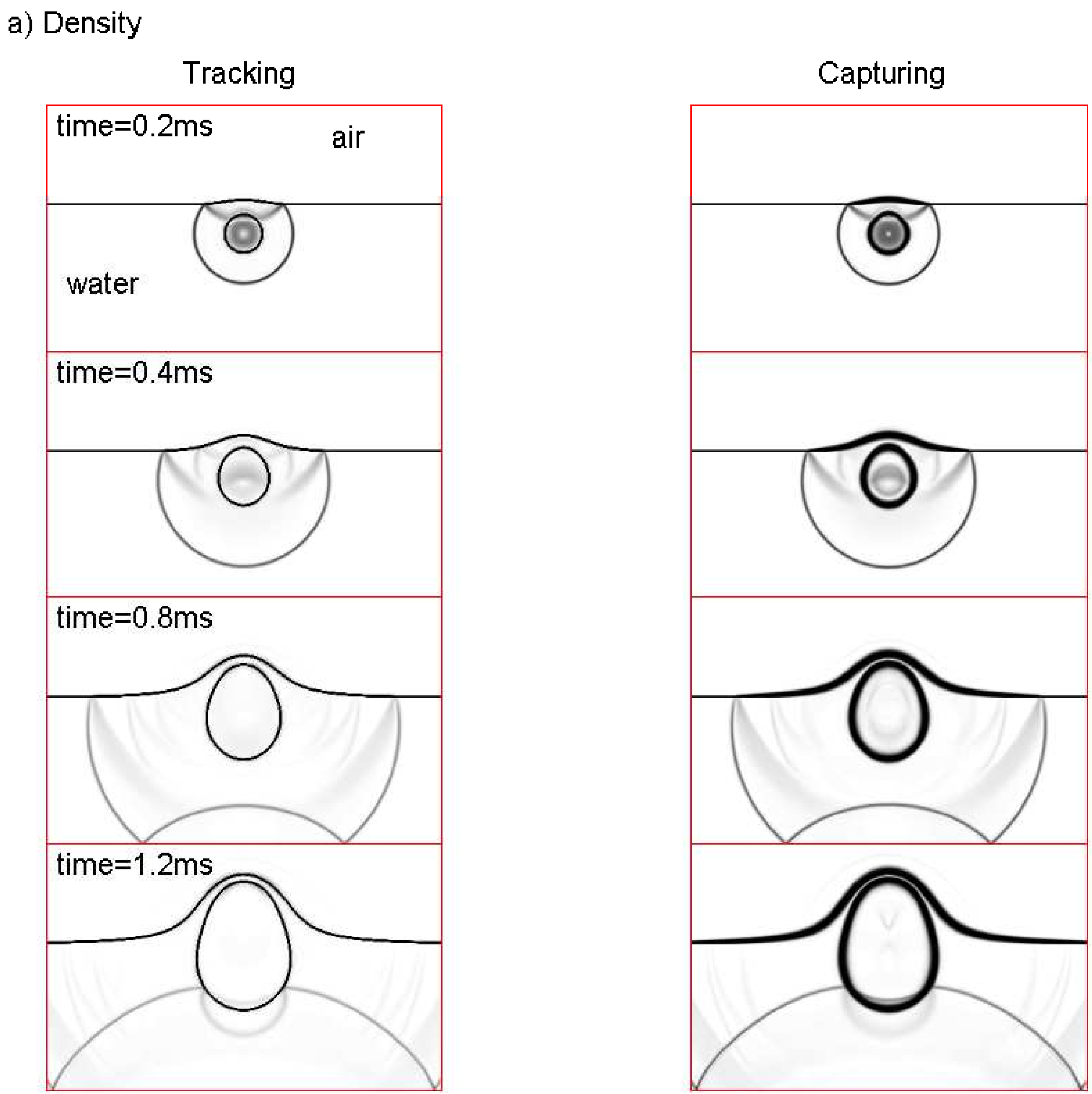

Shock Wave in Bubbly Flow

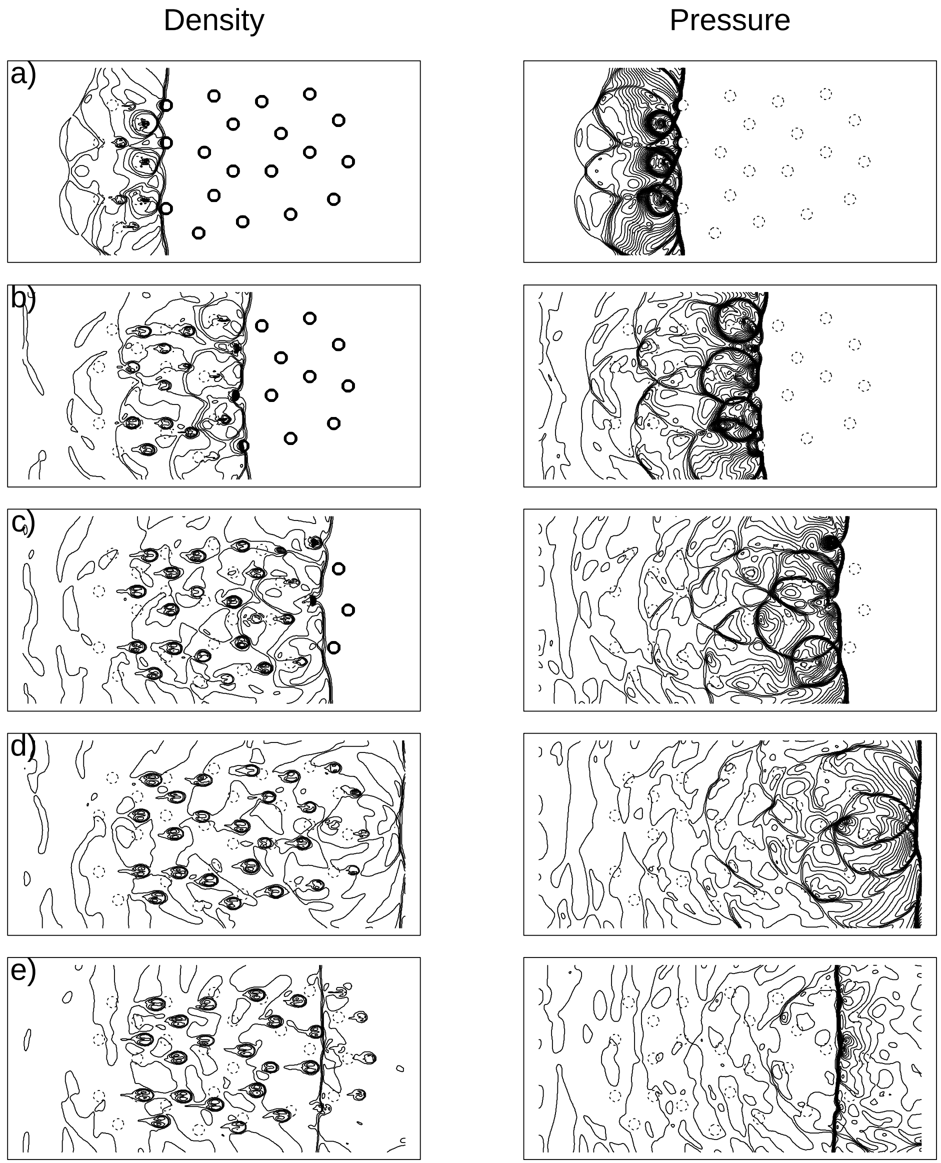

Two-Phase Flow Model

- Saurel & Gallouet (1998)

$$(\alpha_1\rho_1)_t + \nabla\cdot(\alpha_1\rho_1\vec{u}_1) = \dot{m}$$

$$(\alpha_1\rho_1\vec{u}_1)_t + \nabla\cdot(\alpha_1\rho_1\vec{u}_1\otimes\vec{u}_1) + \nabla(\alpha_1 p_1) = p_0\nabla\alpha_1 + \dot{m}\vec{u}_0 + F_d$$

$$(\alpha_1\rho_1 E_1)_t + \nabla\cdot(\alpha_1\rho_1 E_1\vec{u}_1 + \alpha_1 p_1\vec{u}_1) = p_0\left(\alpha_2\right)_t + \dot{m}E_0 + F_d\vec{u}_0 + Q$$

$$(\alpha_2\rho_2)_t + \nabla\cdot(\alpha_2\rho_2\vec{u}_2) = -\dot{m}$$

$$(\alpha_2\rho_2\vec{u}_2)_t + \nabla\cdot(\alpha_2\rho_2\vec{u}_2\otimes\vec{u}_2) + \nabla(\alpha_2 p_2) = p_0\nabla\alpha_2 - \dot{m}\vec{u}_0 - F_d$$

$$(\alpha_2\rho_2 E_2)_t + \nabla\cdot(\alpha_2\rho_2 E_2\vec{u}_2 + \alpha_2 p_2\vec{u}_2) = -p_0\left(\alpha_2\right)_t - \dot{m}E_0 - F_d\vec{u}_0 -$$

$$(\alpha_2)_t + \vec{u}_0\cdot\nabla\alpha_2 = \mu\left(p_2 - p_1\right)$$

$\alpha_k = V_k/V$, $\quad p_k = \rho_k R_k T_k$, $\quad E_k = e_k + \vec{u}_k^2/2$, for $k = 1, 2$
$\rho = \sum_k \alpha_k\rho_k$, $\quad p = \sum_k \alpha_k p_k$

Two-Phase Flow Model (Cont.)

- Model is derived using averaging theory of Drew (Theory of Multicomponent Fluids, D.A. Drew & S. L. Passman, Springer, 1999)

Namely, introduce indicator function χ_k as

$$\chi_k(M,t) = \begin{cases} 1 & \text{if } M \text{ belongs to the phase } k \\ 0 & \text{otherwise} \end{cases}$$

Denote $<\psi>$ as volume averaged for flow variable ψ,

$$\langle\psi\rangle = \frac{1}{V}\int_V \psi \, dV$$

Gauss& Leibnitz rules

$$\langle\chi_k \nabla\psi\rangle = \langle\nabla(\chi_k\psi)\rangle - \langle\psi\nabla\chi_k\rangle \quad \& \quad \langle\chi_k\psi_t\rangle = \langle(\chi_k\psi)_t\rangle - \langle\psi(\chi_k)_t\rangle$$

Two-Phase Flow Model (Cont.)

Take product of each balance law with χ_k, and perform averaging process. In case of mass conservation equation, for example, we have

$$\langle \chi_k \rho_k \rangle_t + \nabla\cdot < \chi_k \rho_k \vec{u}_k >= \langle \rho_k (\chi_k)_t + \rho_k \vec{u}_k \cdot \nabla \chi_k \rangle$$

Since χ_k is governed by

$$(\chi_k)_t + \vec{u}_0 \cdot \nabla \chi_k = 0,$$

yielding the averaged equation for mass

$$\langle \chi_k \rho_k \rangle_t + \nabla\cdot < \chi_k \rho_k \vec{u}_k >= \langle \rho_k \left(\vec{u}_k - \vec{u}_0 \right) \cdot \nabla \chi_k \rangle$$

Analogously, we may derive averaged equation for momentum, energy, & entropy (not shown here)

Two-Phase Flow Model (Cont.)

In summary,

$$
\begin{aligned}
&\langle \chi_k \rangle_t + \langle \vec{u}_k \cdot \nabla \chi_k \rangle = \langle (\vec{u}_k - \vec{u}_0) \cdot \nabla \chi_k \rangle \\
&\langle \chi_k \rho_k \rangle_t + \nabla \cdot < \chi_k \rho_k \vec{u}_k >= \langle \rho_k \left(\vec{u}_k - \vec{u}_0 \right) \cdot \nabla \chi_k \rangle \\
&\langle \chi_k \rho_k \vec{u}_k \rangle_t + \nabla \cdot < \chi_k \rho_k \vec{u}_k \otimes \vec{u}_k > + \nabla \langle \chi_k p_k \rangle = \langle p_k \nabla \chi_k \rangle + \\
&\qquad\qquad \langle \rho_k \vec{u}_k \left(\vec{u}_k - \vec{u}_0 \right) \cdot \nabla \chi_k \rangle \\
&\langle \chi_k \rho_k E_k \rangle_t + \nabla \cdot < \chi_k \rho_k E_k \vec{u}_k + \chi_k p_k \vec{u}_k >= \langle p_k \vec{u}_k \cdot \nabla \chi_k \rangle + \\
&\qquad\qquad \langle \rho_k E \left(\vec{u}_k - \vec{u}_0 \right) \cdot \nabla \chi_k \rangle
\end{aligned}
$$

Note existence of various interfacial source terms, & modelling of these terms is essential and is a difficult issues of multiphase flows

Baer-Nunziato Two-Phase Flow Model

- Baer & Nunziato (J. Multiphase Flow 1986)

$$(\alpha_1\rho_1)_t + \nabla\cdot(\alpha_1\rho_1\vec{u}_1) = 0$$

$$(\alpha_1\rho_1\vec{u}_1)_t + \nabla\cdot(\alpha_1\rho_1\vec{u}_1\otimes\vec{u}_1) + \nabla(\alpha_1 p_1) = p_0\nabla\alpha_1 + \lambda(\vec{u}_2-\vec{u}_1)$$

$$(\alpha_1\rho_1 E_1)_t + \nabla\cdot(\alpha_1\rho_1 E_1\vec{u}_1 + \alpha_1 p_1\vec{u}_1) = p_0\,(\alpha_2)_t + \lambda\vec{u}_0\cdot(\vec{u}_2-\vec{u}_1)$$

$$(\alpha_2\rho_2)_t + \nabla\cdot(\alpha_2\rho_2\vec{u}_2) = 0$$

$$(\alpha_2\rho_2\vec{u}_2)_t + \nabla\cdot(\alpha_2\rho_2\vec{u}_2\otimes\vec{u}_2) + \nabla(\alpha_2 p_2) = p_0\nabla\alpha_2 - \lambda(\vec{u}_2-\vec{u}_1)$$

$$(\alpha_2\rho_2 E_2)_t + \nabla\cdot(\alpha_2\rho_2 E_2\vec{u}_2 + \alpha_2 p_2\vec{u}_2) = -p_0\,(\alpha_2)_t - \lambda\vec{u}_0\cdot(\vec{u}_2-\vec{u}_1)$$

$$(\alpha_2)_t + \vec{u}_0\cdot\nabla\alpha_2 = \mu\,(p_2-p_1)$$

$\alpha_k = V_k/V$: volume fraction ($\alpha_1+\alpha_2=1$), ρ_k: density, $\vec{u}_k$: velocity, p_k: pressure, $E_k = e_k + \vec{u}_k^2/2$: specific total energy, e_k: specific internal energy, $k=1,2$

Baer-Nunziato Model (Cont.)

p_0 & $\vec{u}_0$: interfacial pressure & velocity

- Baer & Nunziato (1986)
  - $p_0 = p_2, \quad \vec{u}_0 = \vec{u}_1$
- Saurel & Abgrall (1999)
  - $p_0 = \sum_{k=1}^{2} \alpha_k p_k, \quad \vec{u}_0 = \sum_{k=1}^{2} \alpha_k \rho_k \vec{u}_k \Big/ \sum_{k=1}^{2} \alpha_k \rho_k$

λ & μ (> 0): relaxation parameters that determine rates at which velocities and pressures of two phases reach equilibrium

Mathematical Structure

- Balance Laws with non-conservative products
- Stiff relaxation term
- Complicated Riemann problem solutions when the model system is hyperbolic
- Reduced model when $\lambda \to 0$, $\mu \to 0$ or $\lambda \to \infty$, $\mu \to \infty$ is popular in practice

Reduced Two-Phase Flow Model

- Murrone & Guillard (JCP 2005)
  - Assume $\lambda = \lambda^{'}/\varepsilon$ & $\mu = \mu^{'}/\varepsilon$, $\lambda^{'} = O(1)$ & $\mu^{'} = O(1)$
  - Use formal asymptotic analysis to show that when $\varepsilon \to 0$ leading order approximation of two-phase flow model takes

$$(\alpha_1\rho_1)_t + \nabla\cdot(\alpha_1\rho_1\vec{u}) = 0$$

$$(\alpha_2\rho_2)_t + \nabla\cdot(\alpha_2\rho_2\vec{u}) = 0$$

$$(\rho\vec{u})_t + \nabla\cdot(\rho\vec{u}\otimes\vec{u}) + \nabla p = 0$$

$$(\rho E)_t + \nabla\cdot(\rho E\vec{u} + p\vec{u}) = 0$$

$$(\alpha_2)_t + \vec{u}\cdot\nabla\alpha_2 = \alpha_1\alpha_2\left(\frac{\rho_1 c_1^2 - \rho_2 c_2^2}{\sum_{k=1}^{2}\alpha_k\rho_k c_k^2}\right)\nabla\cdot\vec{u}$$

Reduced Two-Phase Flow Model (Cont.)

Some remarks about the reduced model:

1. It can be shown entropy of each phase $\mathcal{S}_k$ now satisfies

$$\frac{D\mathcal{S}_k}{Dt} = \frac{\partial \mathcal{S}_k}{\partial t} + \vec{u} \cdot \nabla \mathcal{S}_k = 0, \quad \text{for} \quad k = 1, 2$$

2. Since product $\alpha_1 \alpha_2$ is expected to be small, Shyue (JCP 1998), Allaire, Clerc, & Kokh (JCP 2002) proposed to use

$$(\alpha_2)_t + \vec{u} \cdot \nabla \alpha_2 = 0$$

and now phase entropies satisfy

$$\left(\frac{\partial p_1}{\partial \mathcal{S}_1}\right)_{\rho_1} \frac{D\mathcal{S}_1}{Dt} - \left(\frac{\partial p_2}{\partial \mathcal{S}_2}\right)_{\rho_2} \frac{D\mathcal{S}_2}{Dt} = \left(\rho_1 c_1^2 - \rho_2 c_2^2\right) \nabla \cdot \vec{u}$$

Reduced Two-Phase Flow Model (Cont.)

3. Equation of State: $p = p(\alpha_2,\ \alpha_1\rho_1,\ \alpha_2\rho_2,\ \rho e)$
4. Isobaric Closure: $p_1 = p_2 = p$
   - For a class of EOS, explicit formula for p is available (examples are given next)
   - For complex EOS, from $(\alpha_2, \rho_1, \rho_2, \rho e)$ in model equations we recover p by solving

$$p_1(\rho_1, \rho_1 e_1) = p_2(\rho_2, \rho_2 e_2)$$

$$\sum_{k=1}^{2} \alpha_k \rho_k e_k = \rho e$$

Reduced Two-Phase Flow Model (Cont.)

- Polytropic Ideal Gas: $p_k = (\gamma_k - 1)\rho_k e_k$

$$\rho e = \sum_{k=1}^{2} \alpha_k \rho_k e_k = \sum_{k=1}^{2} \alpha_k \frac{p}{\gamma_k - 1} \quad \Longrightarrow \quad p = \rho e \Big/ \sum_{k=1}^{2} \frac{\alpha_k}{\gamma_k - 1}$$

- van der Waals Gas: $p_k = (\frac{\gamma_k - 1}{1 - b_k \rho_k})(\rho_k e_k + a_k \rho_k^2) - a_k \rho_k^2$

$$\rho e = \sum_{k=1}^{2} \alpha_k \rho_k e_k = \sum_{k=1}^{2} \alpha_k \left[\left(\frac{1 - b_k \rho_k}{\gamma_k - 1} \right) (p + a_k \rho_k^2) - a_k \rho_k^2 \right] \quad \Longrightarrow$$

$$p = \left[\rho e - \sum_{k=1}^{2} \alpha_k \left(\frac{1 - b_k \rho_k}{\gamma_k - 1} - 1 \right) a_k \rho_k^2 \right] \Big/ \sum_{k=1}^{2} \alpha_k \left(\frac{1 - b_k \rho_k}{\gamma_k - 1} \right)$$

Reduced Two-Phase Flow Model (Cont.)

- Two-Molecular Vibrating Gas: $p_k = \rho_k R_k T(e_k)$, T satisfies

$$e = \frac{RT}{\gamma - 1} + \frac{RT_{\text{vib}}}{\exp\left(T_{\text{vib}}/T\right) - 1}$$

As before, we now have

$$\rho e = \sum_{k=1}^{2} \alpha_k \rho_k e_k = \sum_{k=1}^{2} \alpha_k \left[\left(\frac{\rho_k R_k T_k}{\gamma_k - 1} \right) + \frac{\rho_k R_k T_{\text{vib},k}}{\exp\left(T_{\text{vib},k}/T_k\right) - 1} \right]$$

$$= \sum_{k=1}^{2} \alpha_k \left[\left(\frac{p}{\gamma_k - 1} \right) + \frac{p_{\text{vib},k}}{\exp\left(p_{\text{vib},k}/p\right) - 1} \right] \quad (\text{Nonlinear})$$

Reduced Two-Phase Flow Model (Cont.)

5. Model system is hyperbolic under suitable thermodynamic stability condition (see below)
6. It is easy to write the model system in unified coordinates
7. In the model $\alpha_2 \neq 0$ or 1, otherwise, either ρ_2 or ρ_1 is not able to recover from $\alpha_2\rho_2$ or $\alpha_1\rho_1$
8. This formulation of model equation would not work when one fluid component is adiabatic, but the other fluid component is not
9. Surely, there are other set of model systems proposed in the literature that are valid in this relaxation limit

Thermodynamic Stability

- Fundamental derivative of gas dynamics

$$\mathcal{G} = -\frac{V}{2}\frac{(\partial^2 p/\partial V^2)_S}{(\partial p/\partial V)_S}, \qquad S: \text{specific entropy}$$

- Assume fluid state satisfy $\mathcal{G} > 0$ for thermodynamic stability, *i.e.*,

$$(\partial^2 p/\partial V^2)_S > 0 \qquad \& \qquad (\partial p/\partial V)_S < 0$$

- $(\partial^2 p/\partial V^2)_S > 0$ means convex EOS
- $(\partial p/\partial V)_S < 0$ means real speed of sound, for

$$c^2 = \left(\frac{\partial p}{\partial \rho}\right)_S = -V^2\left(\frac{\partial p}{\partial V}\right)_S > 0$$

Thermodynamic Stability (Cont.)

- When $\mathcal{G} \leq 0$, there exist nonclassical nonlinear wave & phase transition (active research area)

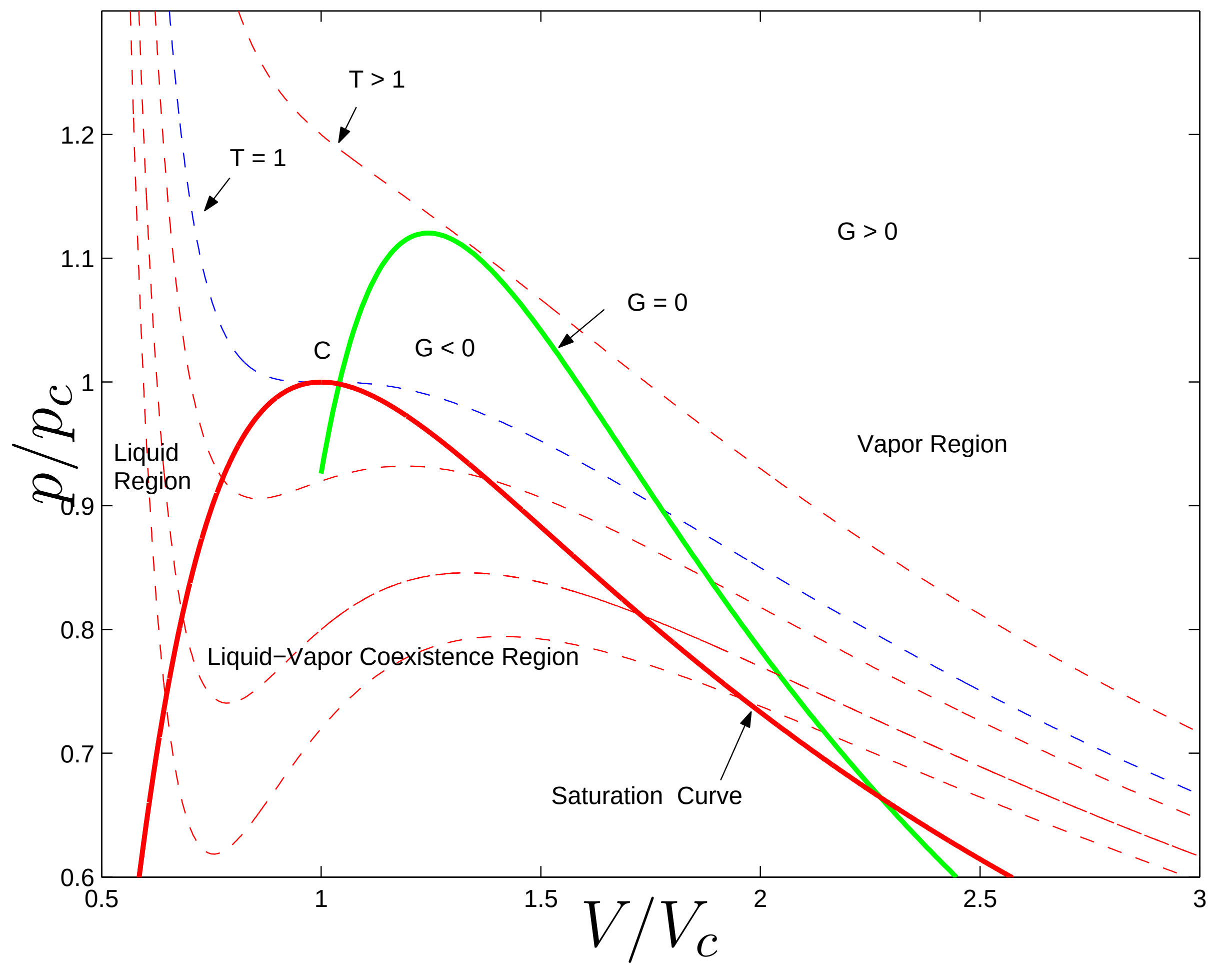

Basic Numerical Approaches

- Method Based on Eulerian Grid
  - Diffuse-interface type
  - Sharp-interface type
- Method Based on Lagrangian Grid
- Method Based on Unified Coordinates
  - Diffuse-interface type
  - Sharp-interface type

Benchmark Test: Interface Only

- Initial Condition

$$\begin{pmatrix} \rho \\ u \\ p \\ \gamma \end{pmatrix}_L = \begin{pmatrix} 1 \\ 1 \\ 1 \\ 1.4 \end{pmatrix} \qquad \& \qquad \begin{pmatrix} \rho \\ u \\ p \\ \gamma \end{pmatrix}_R = \begin{pmatrix} 0.125 \\ 1 \\ 1 \\ 1.2 \end{pmatrix}$$

- Exact Solution

$$\begin{pmatrix} \rho \\ u \\ p \\ \gamma \end{pmatrix}(x,t) = \begin{pmatrix} \rho_0(x-t) \\ 1 \\ 1 \\ \gamma_0(x-t) \end{pmatrix}$$

Benchmark Test (Cont.)

- Eulerian Grid Computations: First order results

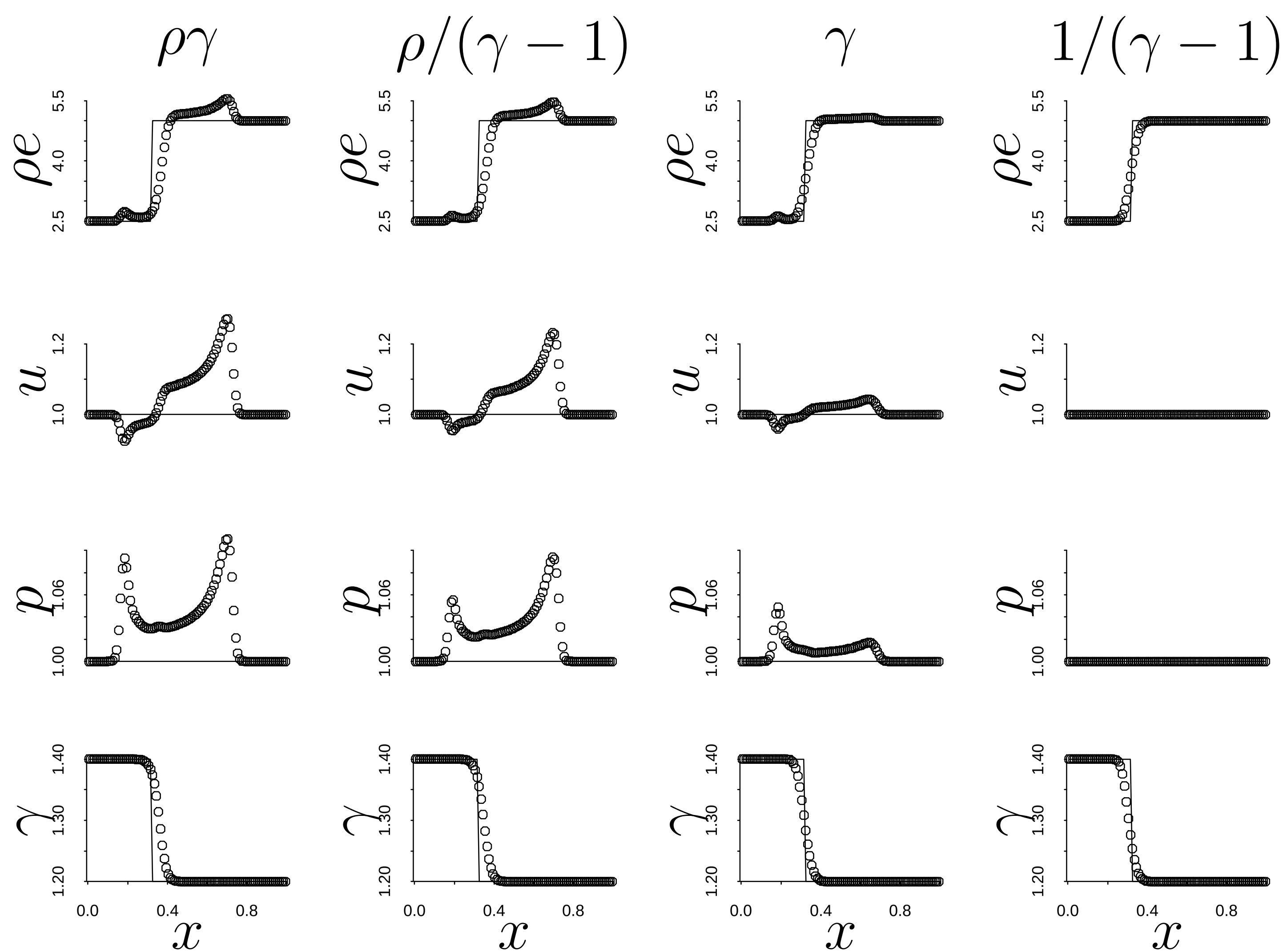

Benchmark Test (Cont.)

- Eulerian Grid Computations: High resolution results

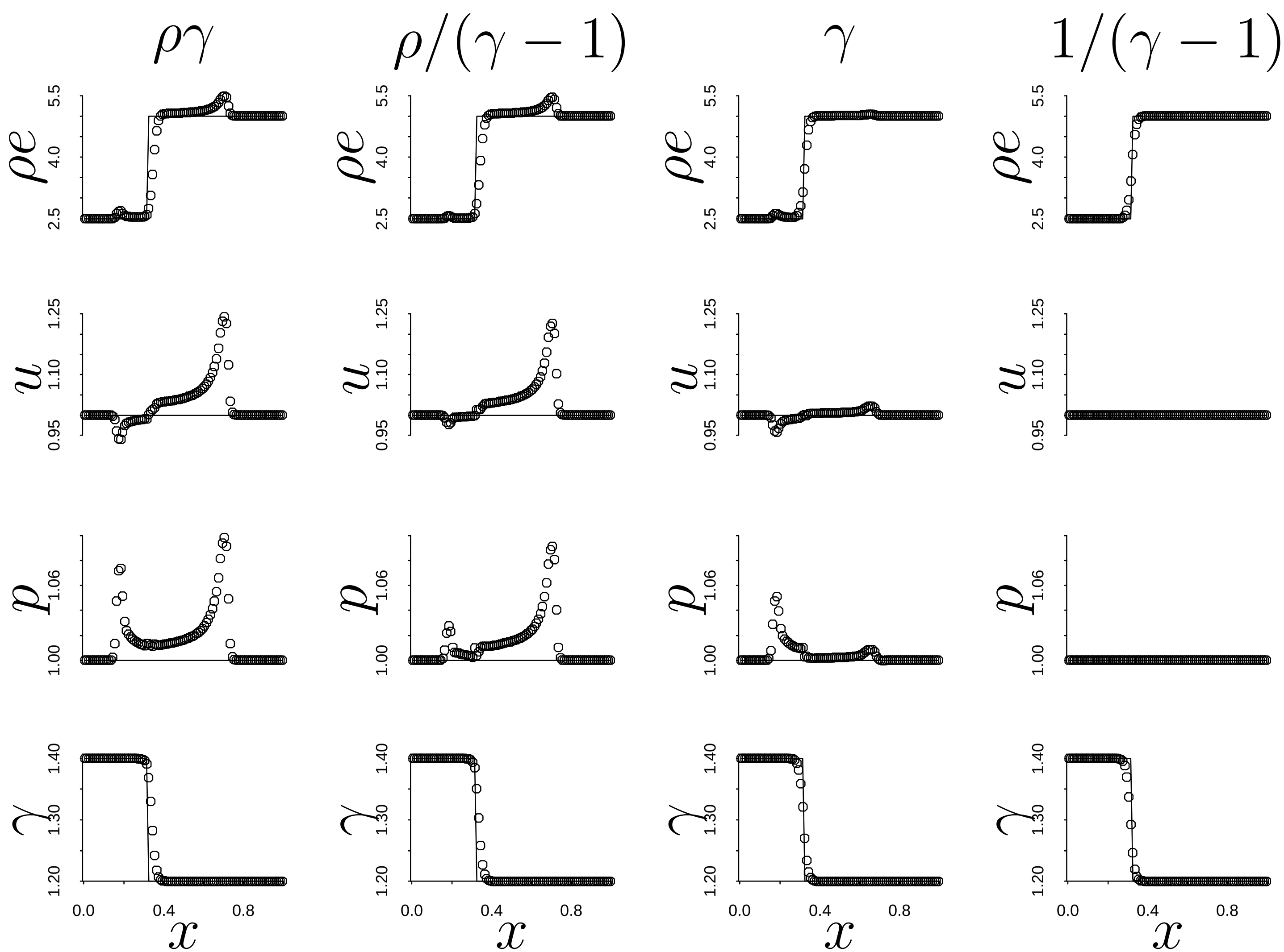

Benchmark Test: Shock-Bubble Interaction

- Eulerian Grid Computations: Density schlieren images

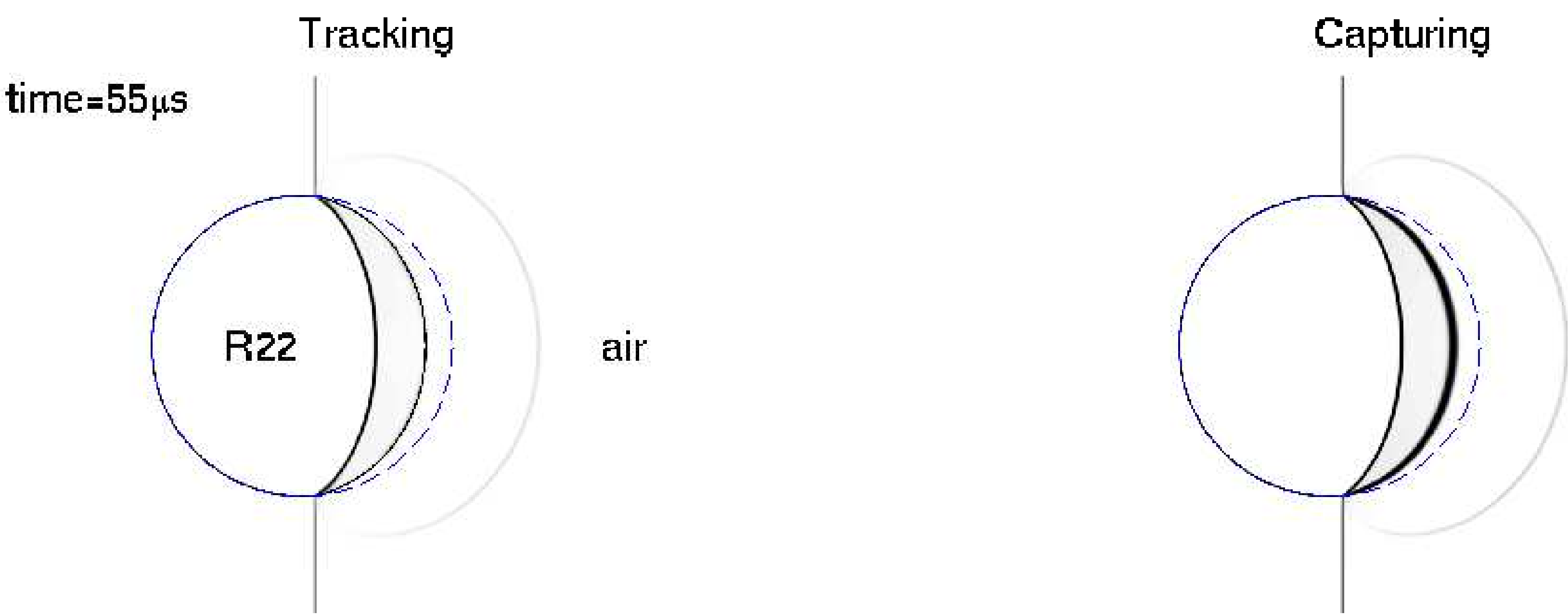

Benchmark Test: Shock-Bubble Interaction

- Eulerian Grid Computations: Density schlieren images

Benchmark Test: Shock-Bubble Interaction

- Eulerian Grid Computations: Density schlieren images

Benchmark Test: Shock-Bubble Interaction

- Eulerian Grid Computations: Density schlieren images

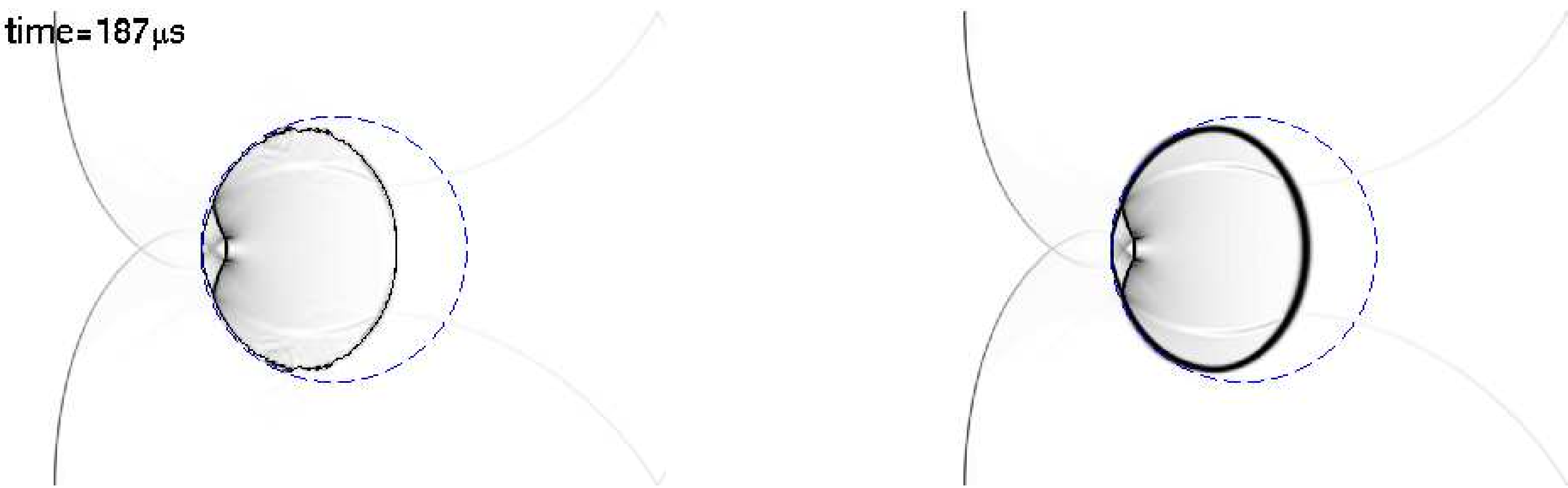

Benchmark Test: Shock-Bubble Interaction

- Eulerian Grid Computations: Density schlieren images

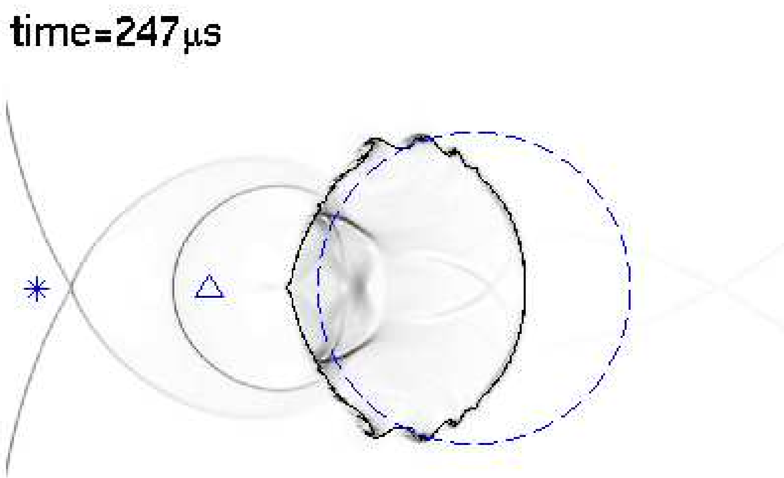

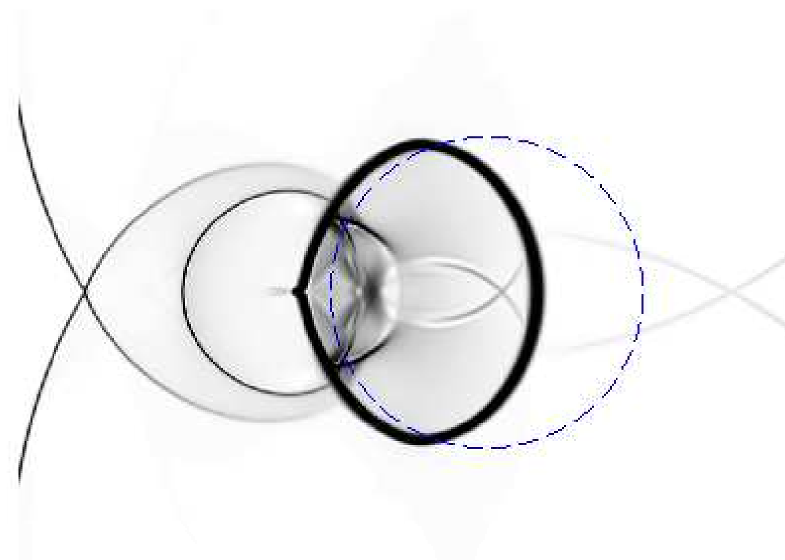

Benchmark Test: Shock-Bubble Interaction

- Eulerian Grid Computations: Density schlieren images

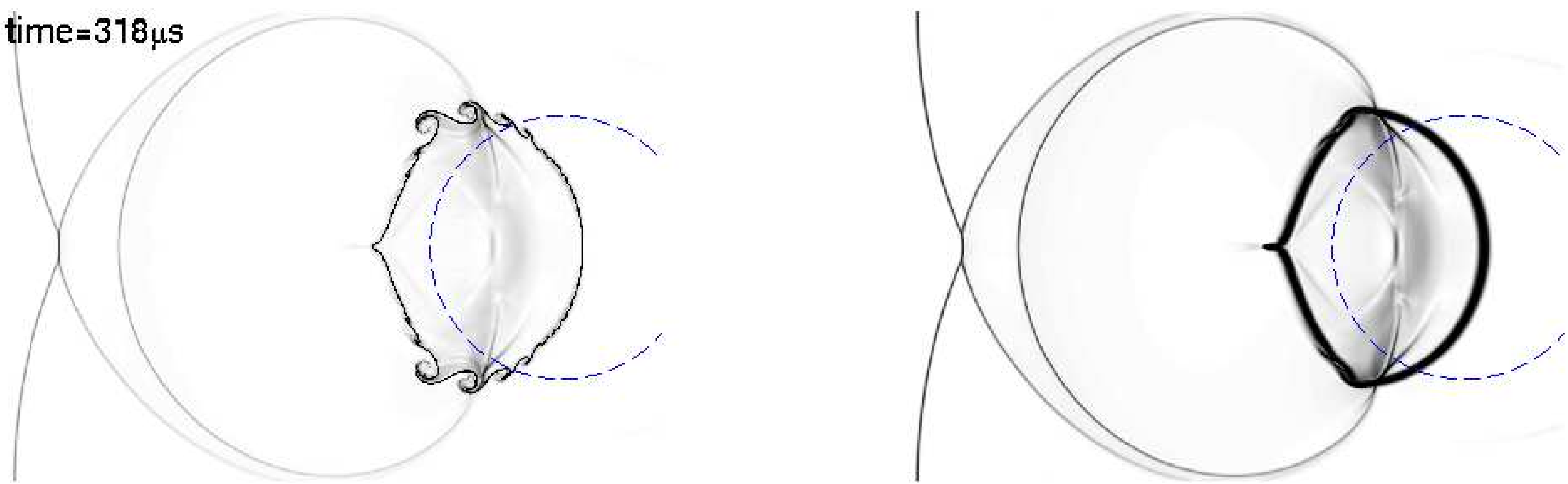

Benchmark Test: Shock-Bubble Interaction

- Eulerian Grid Computations: Density schlieren images

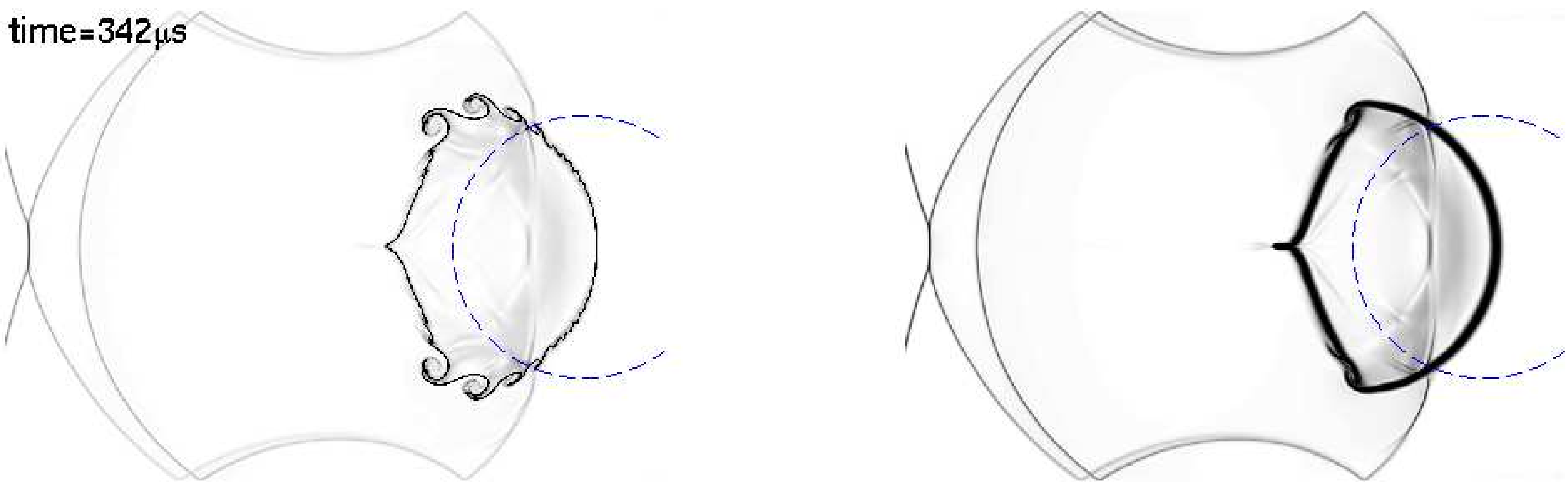

Benchmark Test: Shock-Bubble Interaction

- Eulerian Grid Computations: Density schlieren images

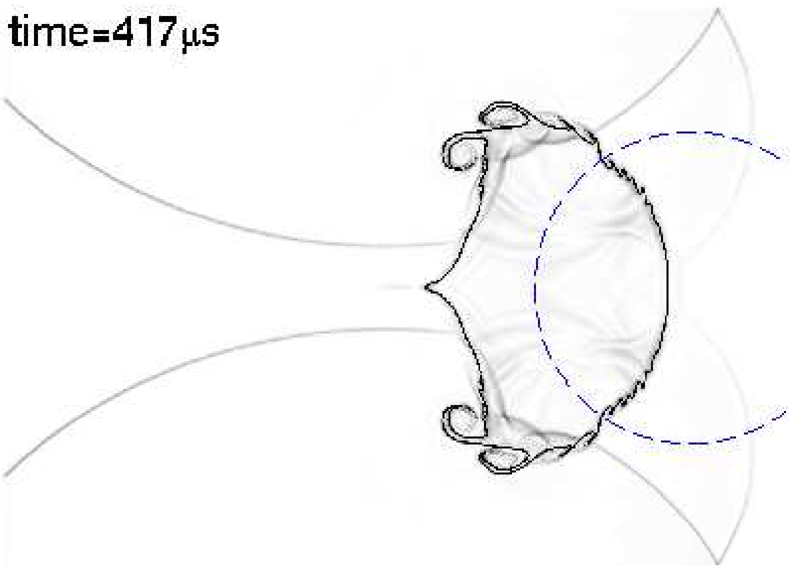

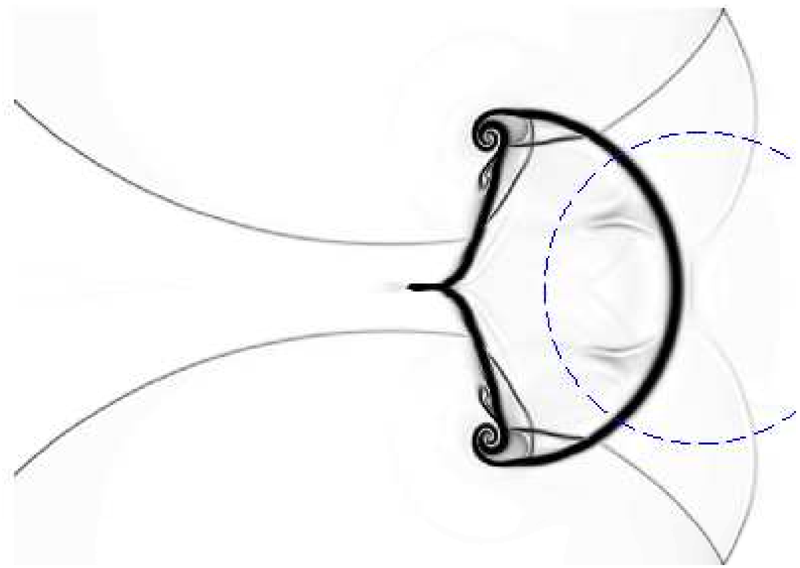

Benchmark Test: Shock-Bubble Interaction

- Eulerian Grid Computations: Density schlieren images

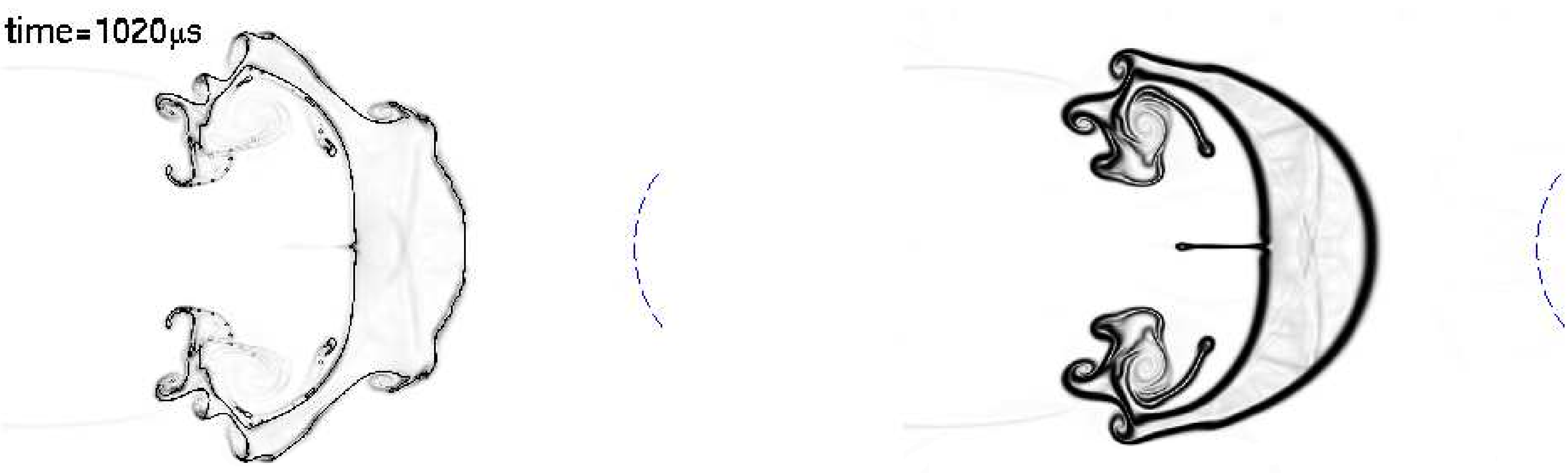

Shock-Bubble Interaction (cont.)

- Approximate locations of interfaces

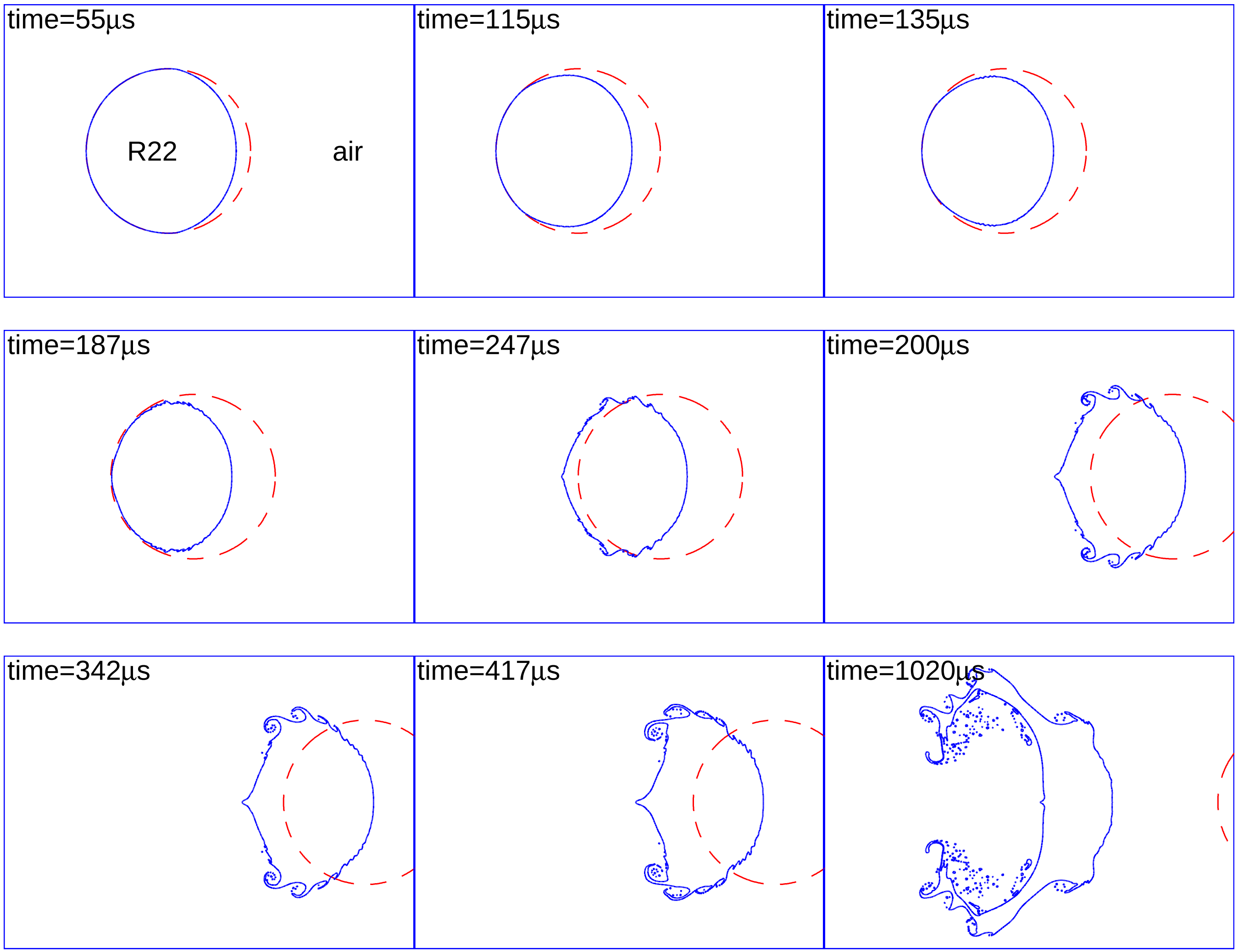

Shock-Bubble Interaction (cont.)

- Comparison of the computed velocities obtained using our tracking and non-tracking algorithms with those reported in the literature

Velocity (m/s)	V_s	V_R	V_T	V_{ui}	V_{uf}	V_{di}	V_{df}
Haas & Sturtevant	415	240	540	73	90	78	78
Quirk & Karni	420	254	560	74	90	116	82
Our result (tracking)	411	243	538	64	87	82	60
Our result (capturing)	411	244	534	65	86	98	76

Shock-Bubble Interaction $3D$

- Eulerian Grid Computations

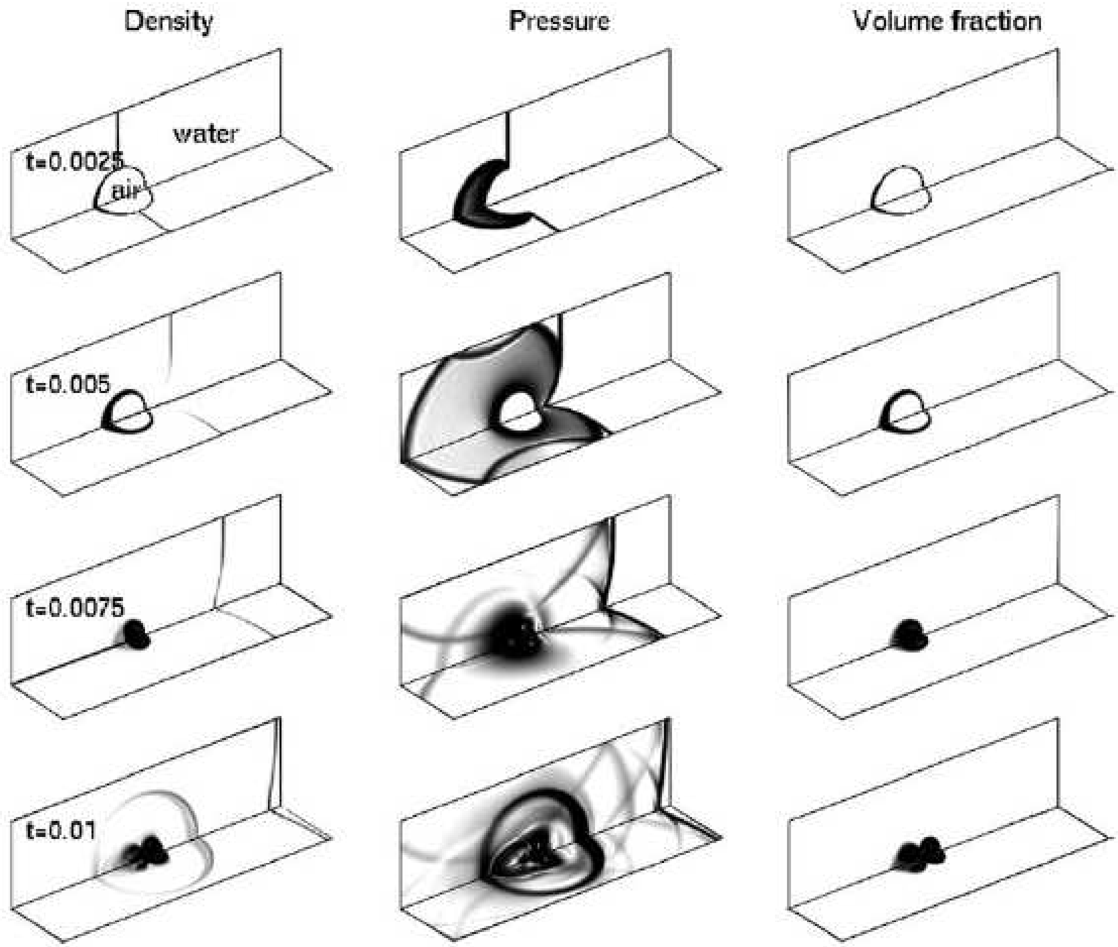

Fig. 12. Three-dimensional results for a planar shock wave in water over an air bubble. Schlieren-type images for the density, pressure, and volume fraction are shown on the planes $y = 0.5$ and $z = 0$ at four different times $t = i \times 0.0025$, for $i = 1, 2, 3, 4$. Here a $400 \times 100 \times 120$ grid was used in the computation.

Shock-Bubble Interaction (cont.)

- Because of the complication in topological structure of interface, it is not clear how to impose the condition

$$\frac{D_Q \eta}{Dt} = 0$$

in unified coordinates

Supersonic NACA0012 over Heavier Gas

- Unified Coordinates Computations

a)

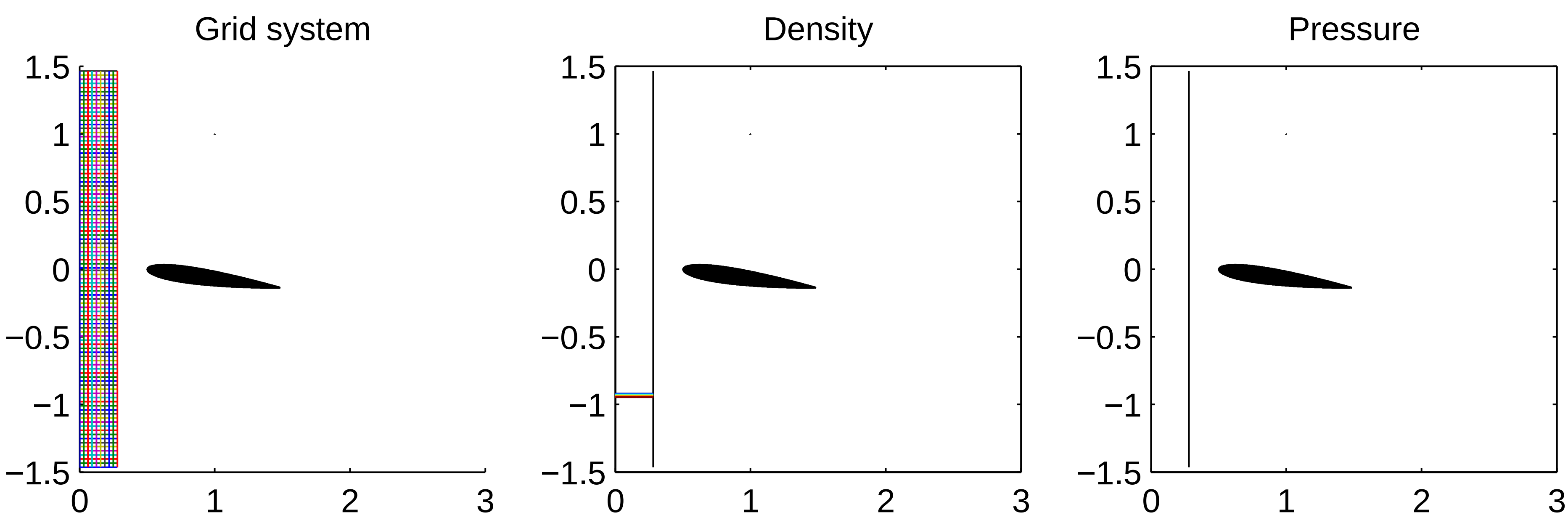

Supersonic NACA0012 over Heavier Gas

- Unified Coordinates Computations

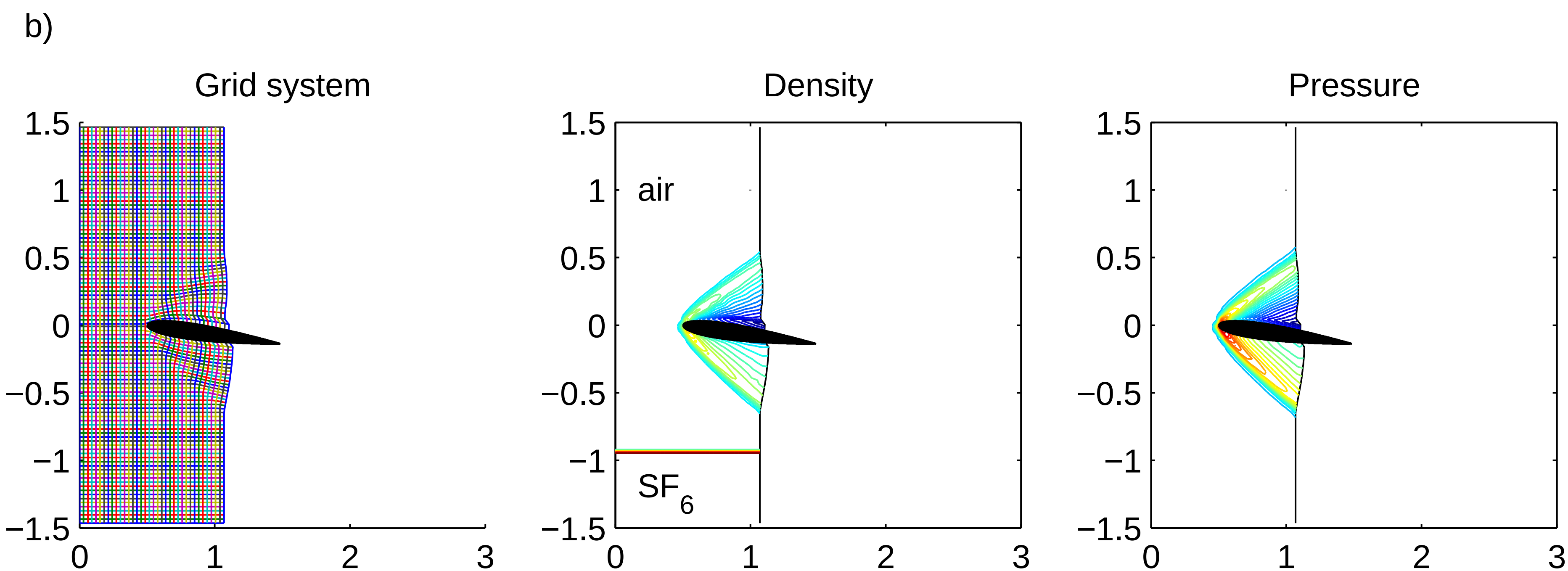

Supersonic NACA0012 over Heavier Gas

- Unified Coordinates Computations

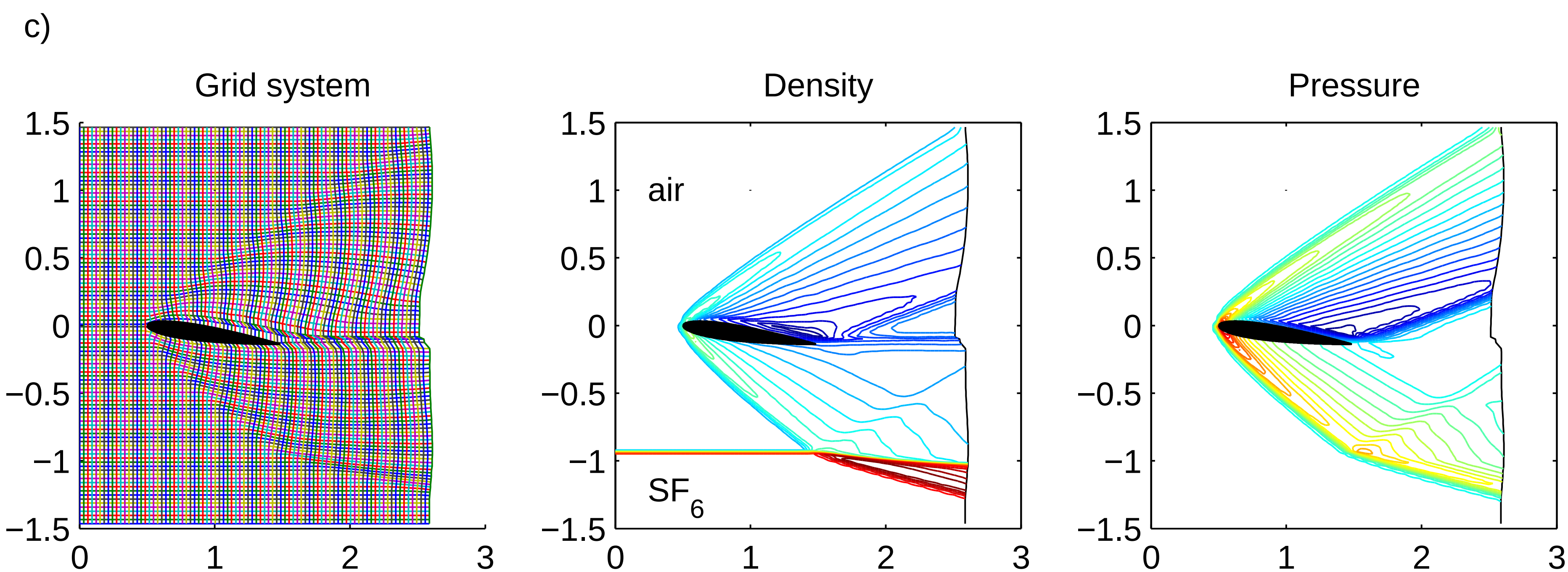

Supersonic NACA0012 over Heavier Gas

- Eulerian Grid Computations

Grid system

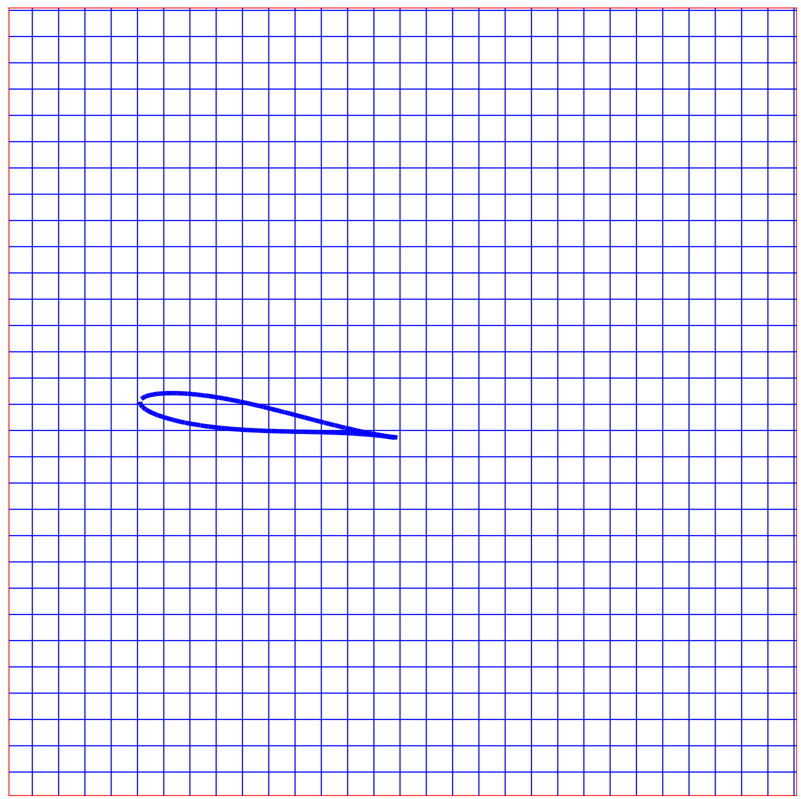

Supersonic NACA0012 over Heavier Gas

- Eulerian Grid Computations

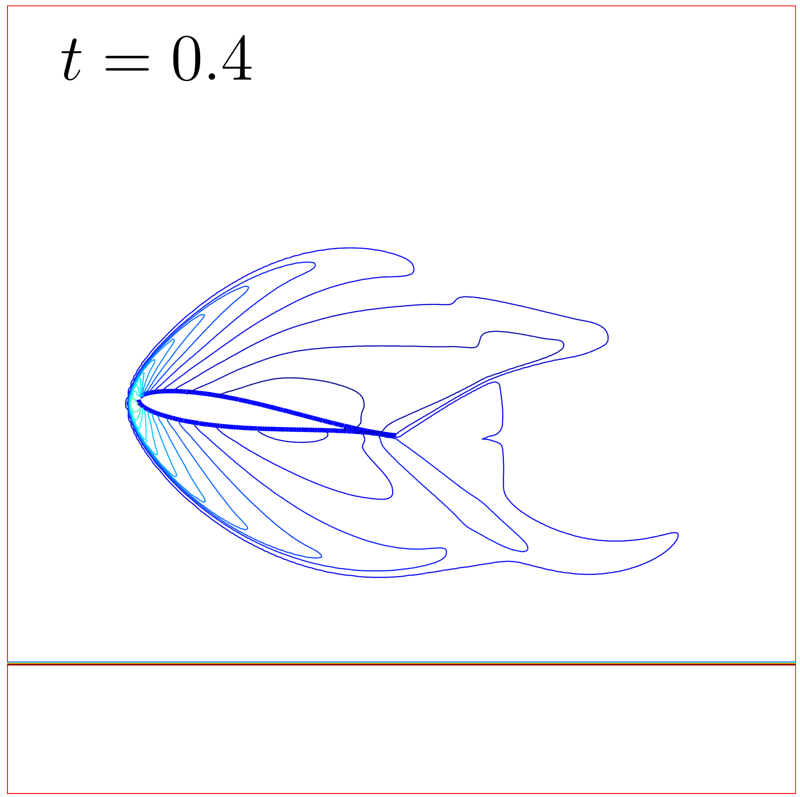

Supersonic NACA0012 over Heavier Gas

- Eulerian Grid Computations

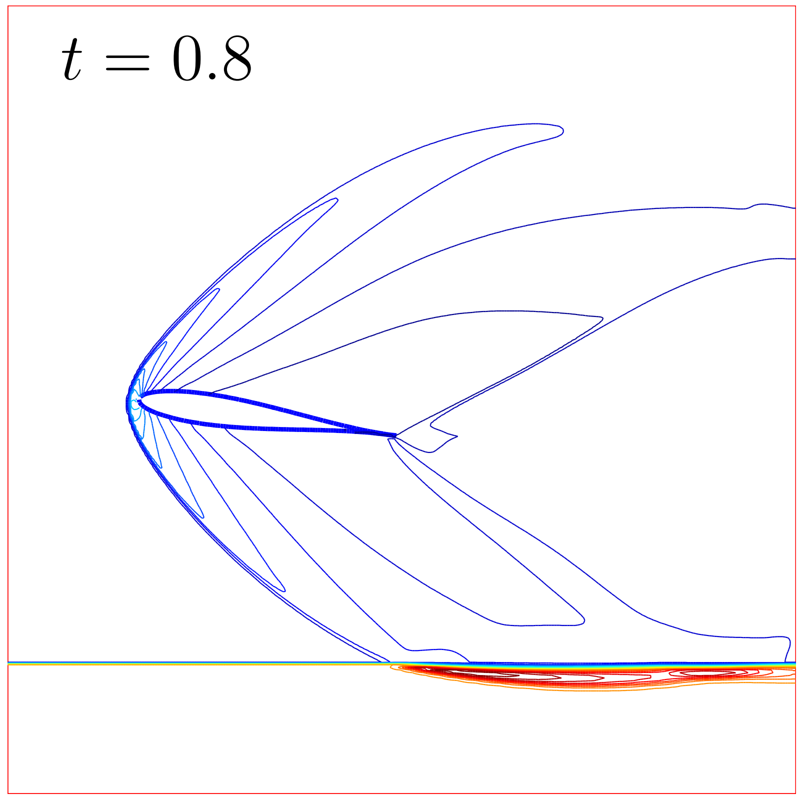

Supersonic NACA0012 over Heavier Gas

- Eulerian Grid Computations

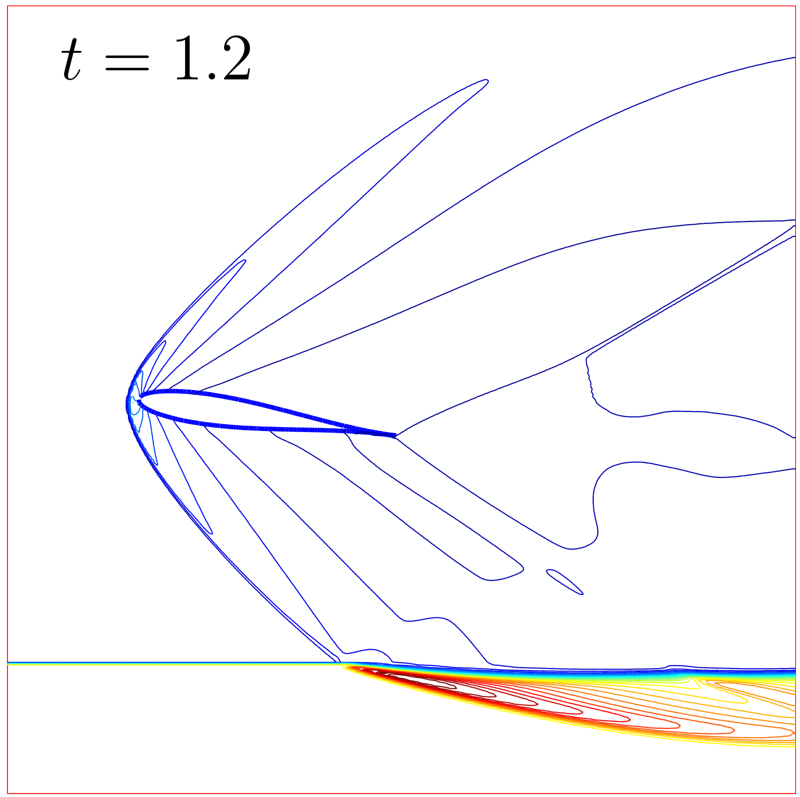

Supersonic NACA0012 over Heavier Gas

- Eulerian Grid Computations

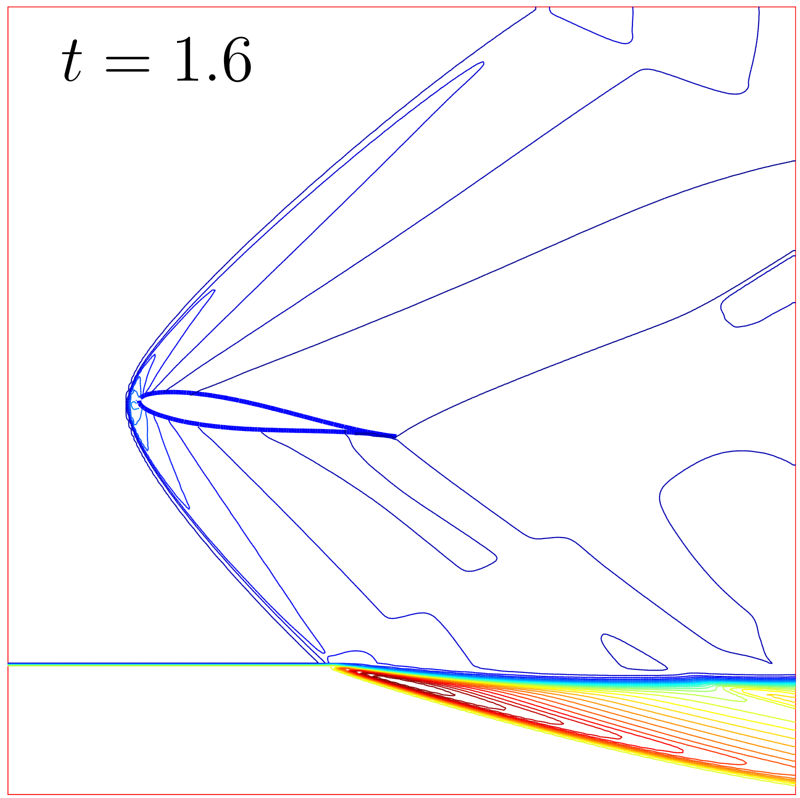

Supersonic NACA0012 over Heavier Gas

- Eulerian Grid Computations

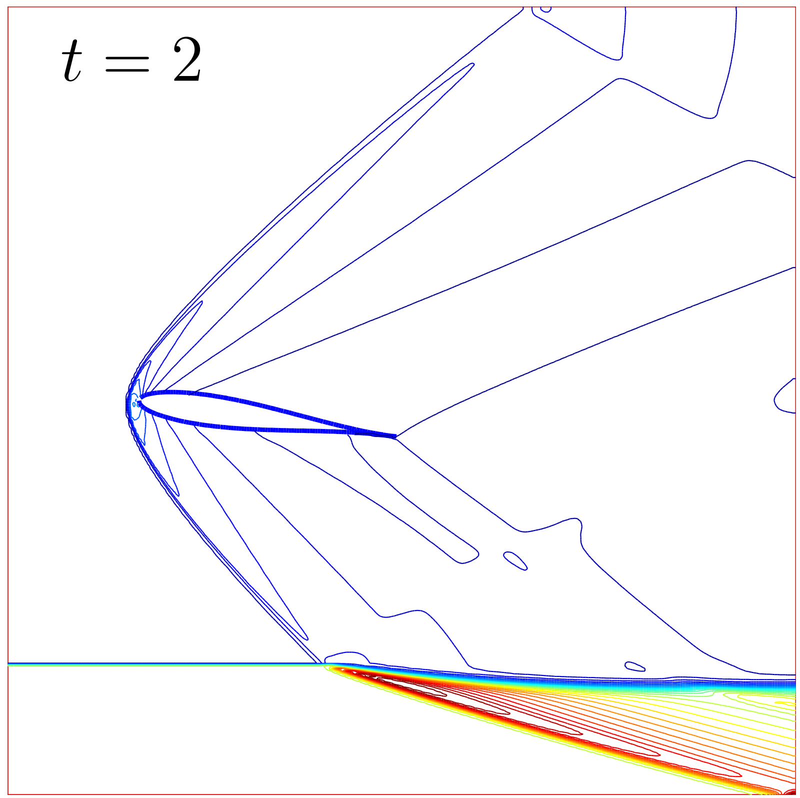

2 Phase Shock over Cylinder

- Eulerian Grid Computations

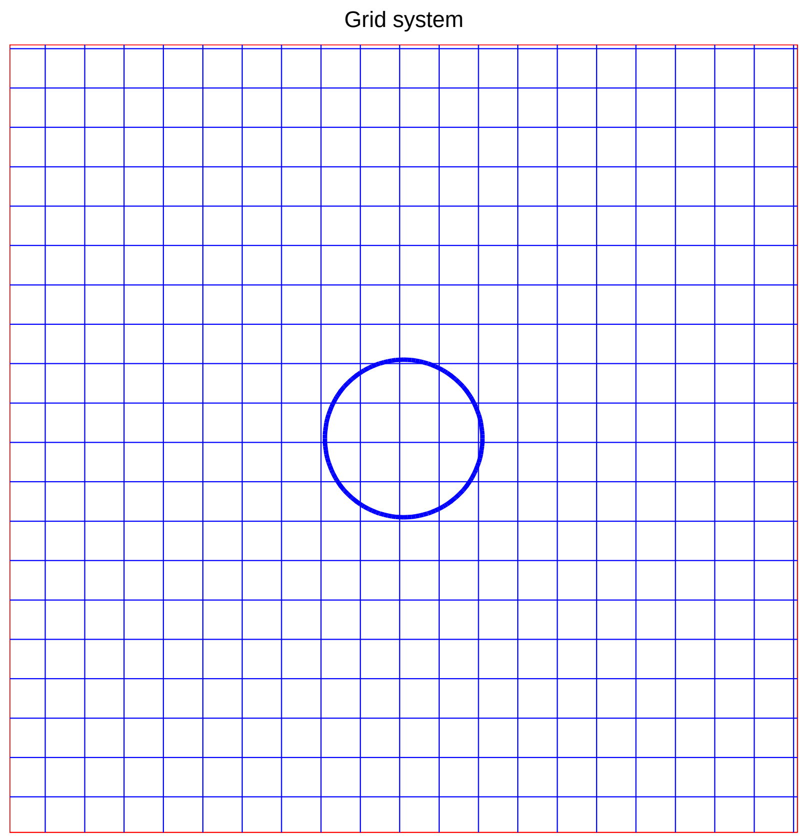

2 Phase Shock over Cylinder

- Eulerian Grid Computations

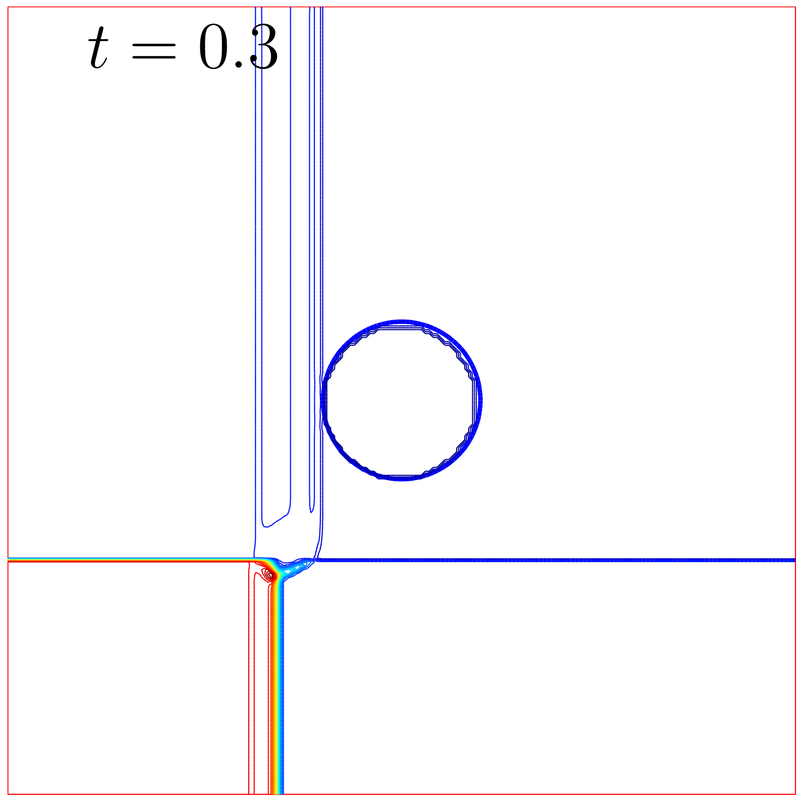

2 Phase Shock over Cylinder

- Eulerian Grid Computations

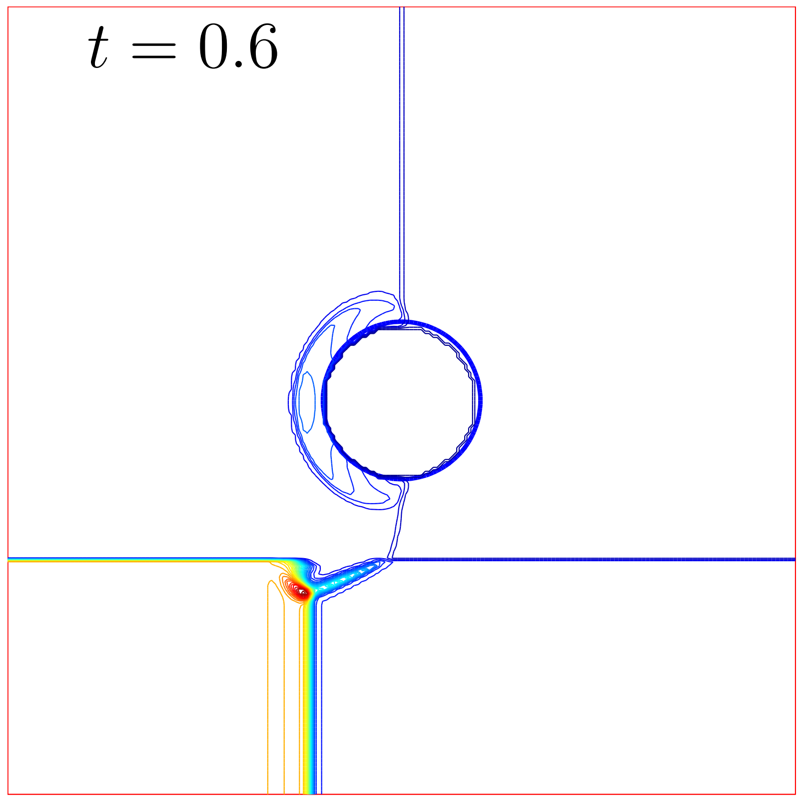

2 Phase Shock over Cylinder

- Eulerian Grid Computations

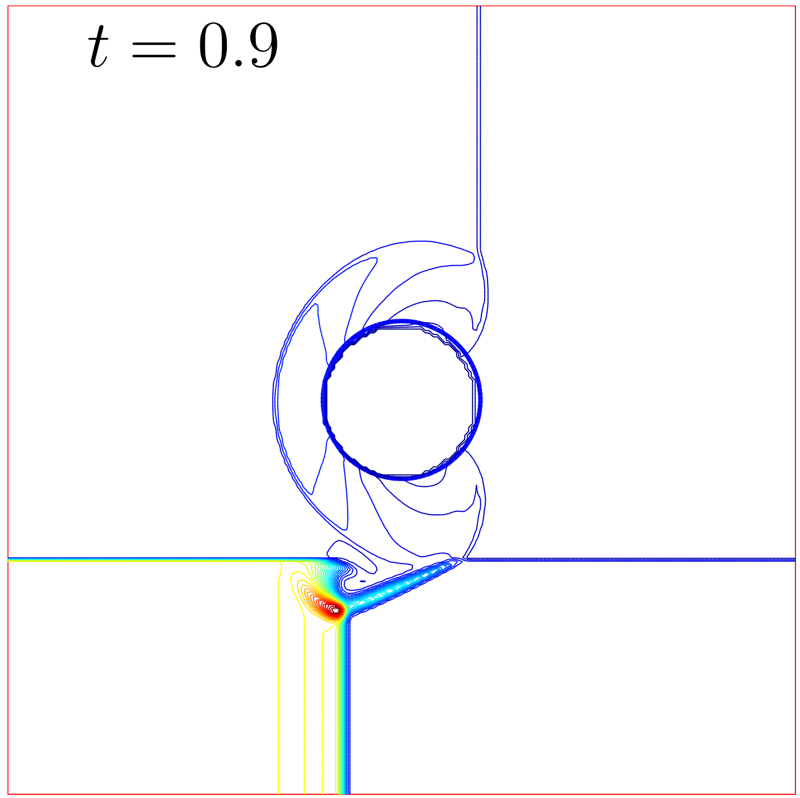

2 Phase Shock over Cylinder

- Eulerian Grid Computations

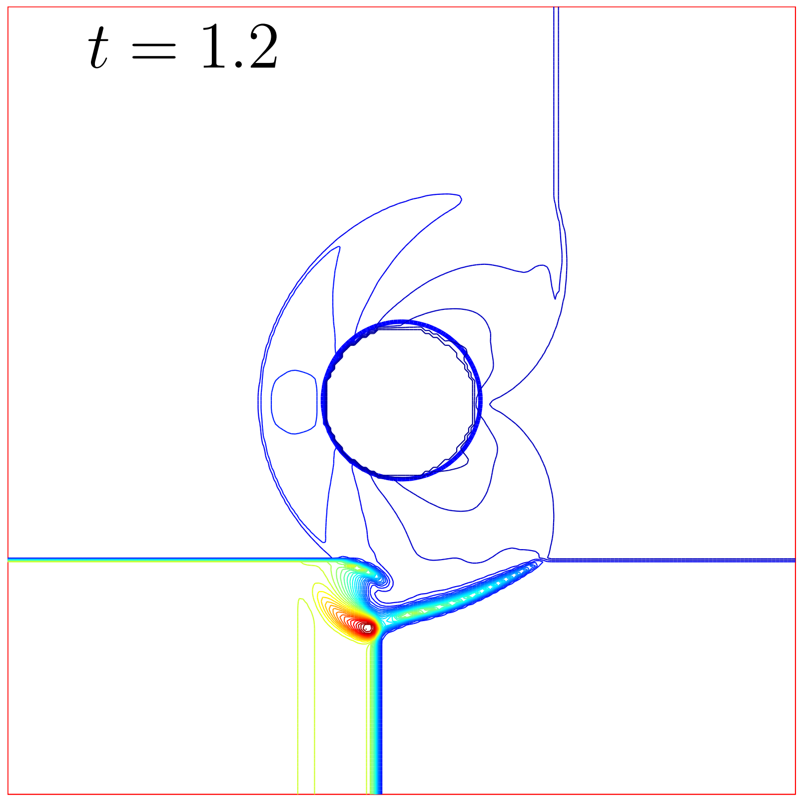

2 Phase Shock over Cylinder

- Eulerian Grid Computations

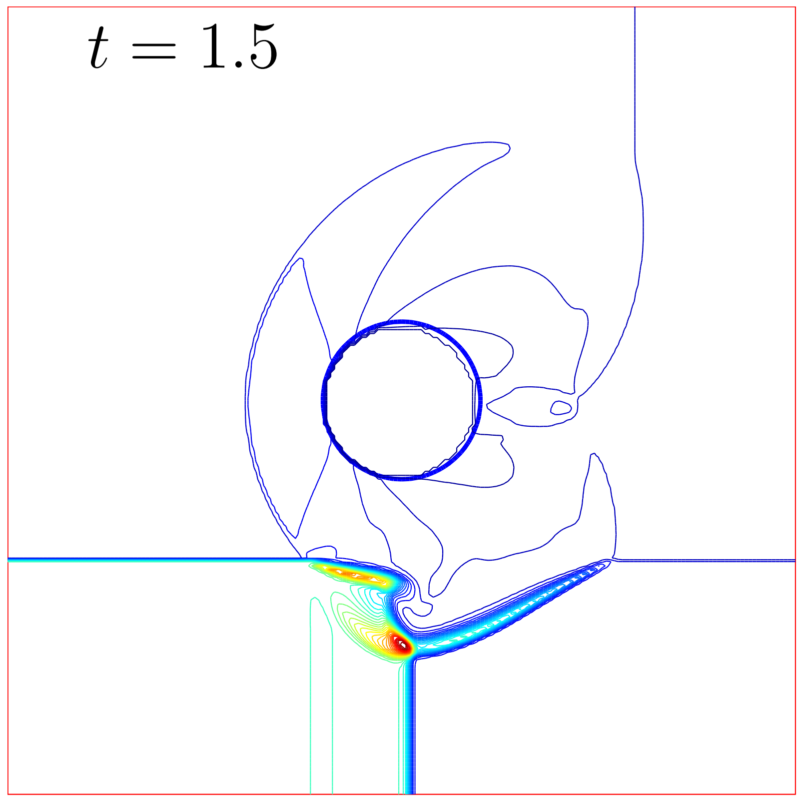

Final Remarks

Potential use of unified coordinates approach in multiphase flow problems are:

- Simple topological structure of interfaces
- Existence of (fixed or moving) boundary
  - Use as a body-fitted grid generation tool
  - Use in a space-marching (flow-generated grid) computations
-

Final Remarks

Potential use of unified coordinates approach in multiphase flow problems are:

- Simple topological structure of interfaces
- Existence of (fixed or moving) boundary
  - Use as a body-fitted grid generation tool
  - Use in a space-marching (flow-generated grid) computations
-

I am currently writting a unified coordinates code with the state-of-the-art numerical method included in 2D. The code will be put in the public domain, when it is done.

Thank You